

Electronic and vibrational spectra of III-VI layered semiconductors

G. L. Belen'kiĭ and V. B. Stopachinskiĭ

*Institute of Physics of the Academy of Sciences of the Azerbaijan SSR
and P. N. Lebedev Physics Institute, Academy of Sciences of the USSR
Usp. Fiz. Nauk 140, 233-270 (June 1983)*

An analysis is made of the many theoretical and experimental studies of layered crystals. The results of this analysis for the particular case of group III-VI semiconductors are used to investigate the features in the electronic and phonon spectra which are due to the manifest structural anisotropy of these compounds. It is shown that in both the phonon and electronic spectra there are branches (bands) in which there is practically no dispersion in the direction of the *C* axis of the crystal. These vibrational branches (the so-called "intralayer vibrations") and energy bands (made up, for example, of the metal orbitals) are extremely anisotropic (quasi-two-dimensional). The intralayer vibrations contribute substantially to the phonon subsystem of layered crystals, and, therefore, all the properties which are determined to an appreciable degree by the phonon subsystem are highly anisotropic. The basic electronic properties of the semiconductors, being determined by the structure of only two bands (the conduction and valence bands), are almost isotropic. The reason for this is that these bands are made up of the p_z orbitals of the metalloid, which, according to theoretical calculations of the electron density distribution, overlap with the corresponding states of the neighboring layers. This conclusion is supported by numerous experimental studies of the exciton spectra and photoemission of III-VI layered semiconductors.

PACS numbers: 71.25.Tn

CONTENTS

1. Introduction	497
2. Crystal structure of group III-VI layered semiconductors	498
3. Phonon spectra of III-VI layered semiconductors	499
4. Effect of lattice anisotropy on the exciton states in layered crystals	503
5. Anisotropy of excitons in gallium selenide	508
6. Electronic charge-density distribution in III-VI layered semiconductors	511
7. Conclusion	514
References	515

1. INTRODUCTION

Layered crystals are typified by an obvious structural anisotropy which leads to a quasi-two-dimensional character of the vibrational states in these materials and is manifested most clearly in all the properties governed by the phonon subsystems of these crystals. Strictly speaking, the presence of a weak coupling between layers in a crystal does not by any means imply that all the electronic states should be extremely anisotropic. Nevertheless, a very large number of experimental physicists have chosen layered semiconductors as objects of study in the hope of verifying some theoretical predictions concerning the course of physical phenomena in crystals with extremely anisotropic electron spectra. Among these theoretical predictions, the most interesting are the ideas of Ginzburg¹ and Little² that systems with extremely anisotropic electron spectra can be used to create a high-temperature superconducting state. However, in spite of the fact that the chemical formulas of the majority of these layered compounds have long been known, extensive studies of the energy spectra of crystals with a layered type of crystal lattice began only 15-20 years ago. The most important reason for this state of affairs is evidently that it was only at that time that the technology had advanced to the point where single-phase samples large

enough to be suitable for various optical measurements became available to researchers. This alone, of course, was not enough. The optical spectra of most layered semiconductors are extremely complex and typically contain a large number of lines. It was at just this time that the complex of methods constituting modulational spectroscopy became nearly complete, permitting extremely reliable interpretation of the optical absorption spectra of layered crystals (in particular, near the fundamental absorption band). The results of these studies could be used by theorists, who by the end of the sixties had considerable computational capacity at their disposal, enabling them to make pseudopotential calculations of the band structure of crystals with more than two atoms in the unit cell, provided that the symmetry of the cell was not too low.

Photoemission studies of the electronic spectra of crystals yielded experimental information on the dispersion of the electron bands of semiconductors in which the cyclotron resonance could not be studied because of short carrier relaxation times.

Thus, it became possible for experimentalists and theorists working in the field of semiconductor physics to obtain sufficiently complete information on the electronic spectra of crystals with a complex crystal structure and a low degree of purity (compared to Ge and Si, at least).

The most intensively studied crystals are III-VI and IV-VI semiconductors,^{3,4} transition-metal dichalcogenides with a layered type of lattice,⁵ crystals such as the mineral orpiment (As_2S_3),⁶ layered compounds of iodine and bismuth,³ and a number of others.

This survey is not intended by the authors to be a systematic and exhaustive exposition of the physical properties of layered crystals in general or even of some particular group. Our purpose is to take the available theoretical and experimental data on the energy spectra of layered semiconductors of a single class and use them to construct a picture of how the presence of weak coupling between the layers is manifested in the vibrational and electronic spectra of these crystals and to discuss the interrelation of the vibrational and electronic spectra of layered semiconductors.

The most important conclusion which follows from an analysis of the experimental data is that in a number of typical layered semiconductors the properties of the exciton spectra at the absorption edge, from which one can judge the properties of the electron bands, are practically no different from the ordinary, well-known properties of the exciton spectra in three-dimensional crystals. In order to understand what was going on, it was necessary to construct maps of the electron density distribution in the layered semiconductor by calculational means and to obtain experimental proof of the validity of the calculations. It turned out that the energy states whose electron density is formed from atomic orbitals which overlap from one layer to the next are located at the boundaries of the conduction and valence bands and dictate an extremely weak anisotropy of excitations with $K=0$ in crystals of the GaSe type.

The current understanding of the interrelation between the features of the crystal structure of layered semiconductors and their energy spectra derives from the work of many physicists. The development of the modern concepts is most successfully demonstrated in the case of III-VI semiconductors.

The progress that has been made in the technology of growing these crystals and the prospects for their technological use^{7,10} have stimulated many studies of the optical properties of semiconductors of the GaSe type and prompted calculations of the band structure of these crystals.¹¹ By now, perhaps, there are enough experimental and theoretical data available on the vibrational and electronic spectra in GaSe that it would be worthwhile to discuss what is known about this subject.

2. CRYSTAL STRUCTURE OF GROUP III-VI LAYERED SEMICONDUCTORS

An example of a crystal structure is graphite, in which each layer consists of a single plane of carbon atoms. The coupling between layers is due to van der Waals forces. The distance between carbon atoms within a graphite layer (1.421 Å) is substantially smaller than the distance between layers (3.3 Å).¹²

All the other known layered crystals have a similar structure, but in each of these a layer contains three or

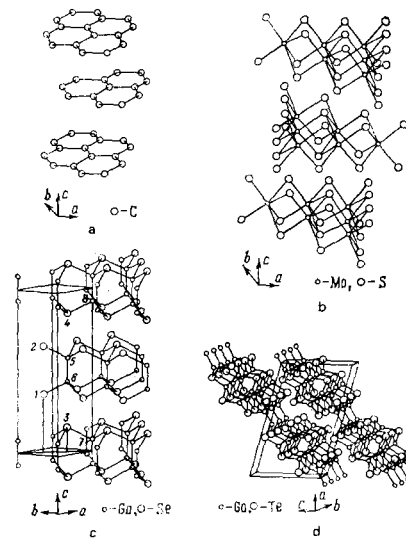


FIG. 1. Crystal structures of various semiconductors with layered lattices (the scale is not consistent). a) Graphite structure; b) MoS_2 structure; c) ϵ -GaSe structure (the unit cell is shown, containing eight atoms from two layers); d) GaTe structure (the monoclinic cell of the crystal is shown).

more planes of atoms. Figure 1 shows sketches of several typical crystal lattices of various layered semiconductors. Binary crystals of the III-VI semiconductor group—GaS, GaSe, and InSe—are made up of layers containing four planes of atoms each. Within the layers the bonding is of an ionic-covalent character, while between layers the interaction is predominantly of the van der Waals type, with a small Coulombic admixture.^{13,14} The structure of the layers is the same in GaS, GaSe, and InSe. The anions and cations are arranged in planes perpendicular to the C axis in the sequence (for GaS, say) S-Ga-Ga-S. The arrangement of atoms within a layer corresponds to space group D_{3h}^1 ($6m2$). Three anions and a metal atom form a tetrahedron (see Fig. 1). Depending on how the layers are stacked, GaSe and InSe can have structures corresponding to various polytypes. The four known polytypes are shown schematically in Fig. 2. The β structure has symmetry space group D_{6h}^4 ($6/mmm$) and, like the ϵ polytype of symmetry D_{3h}^1 , contains two layers in a hexagonal cell. The rhombohedral structure of the γ polytype C_{3v}^3 ($3m$) con-

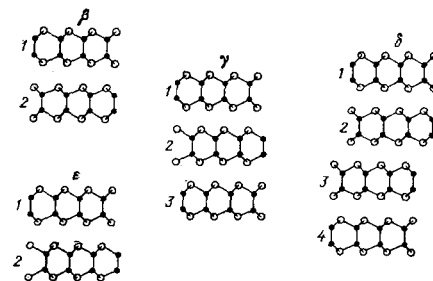


FIG. 2. Schematic representation of various types of stacking of the layers in GaS (β polytype), GaSe (β , ϵ , γ , and δ polytypes), and InSe (β and γ polytypes).

TABLE II.

β polytype Space group D_{6h}^4				ϵ polytype Space group D_{3h}^4				β -InSe		β -GaS		ϵ -GaSe
Raman	IR	Acoust.	Inact.	Raman	IR	Raman, IR	Acoust.	22, 166	22 Inact.	23, 167	22 Inact.	167-169
A_{1g}^1			B_{1u}^1	A_1^1				115	105	188	172	134
A_{1g}^2			B_{1u}^2	A_1^2				225	227	360	353	308
E_{1g}^1			E_{2u}^1	A_1^3				40	38	75	70	60
E_{1g}^2			E_{2u}^2	A_1^4								
E_{2g}^1	E_{1u}^2			E^*1		E^*3		176 Raman		295 Raman		TO { 215 Raman 213 IR
E_{2g}^2		E_{1u}^1		E^*2		E^*4		TO 178 } IR LO 214 }		TO 297 } IR LO 357 }		LO { 252 Raman 254 IR
	A_{2u}^2		B_{2g}^1	E^*3		E^*4		17		22		19.5
		A_{2u}^1	B_{2g}^2	E^*4		E^*2	E^*1	TO 190 LO 200		TO 318 LO 335	328	TO 237 LO 245
									37		55	40

position of the lines in the Raman-scattering spectra.³⁵ The coefficient $\gamma = 1/\omega d\omega/dP$ (ω is the frequency of the mode and P is the pressure at $T = 300$ K) is $20 \cdot 10^{-6}$ bar⁻¹ for the interlayer modes (E_{2g} and E') and 10^{-6} bar⁻¹ for all the other modes, whose frequencies are determined by the forces coupling the atoms within a layer (Fig. 4).

Having determined the values of the interlayer frequencies, one can compare the interlayer interaction with the forces which couple the atoms within the layers in various crystals. Using simple models for the force constants, Zallen and Slade³⁶ estimated separately the constants characterizing the interaction between atoms located within the layers and on the boundaries of the layers. They used different (and rather crude) models for these two cases, but the same models were applied to different crystals. It turned out that the ratio of the

force constants characterizing the interactions between layers (k_0) and between atoms within a layer (the shear constant k_1) was similar in order of magnitude for all the chalcogenides but substantially smaller in graphite. In graphite the atoms within a layer are more strongly coupled than in layered chalcogenide semiconductors (Table III).

The interlayer modes in layered semiconductors can be compared with the low-frequency vibrations in molecular crystals, in which there are also two types of interactions with different magnitudes between different groups of atoms. The concepts and methods that have been developed for the study of the energy spectra of molecular crystals were first used by Zallen and Slade²⁶ and Lisitsa *et al.*²⁷ in analyzing the vibrational spectra of As_2S_3 and As_2Se_3 . This approach has proved extremely useful for describing the experimentally detected splitting of the Raman lines in GaSe. Let us discuss the cause of this splitting. In Fig. 3 the atomic displacement vectors corresponding to the normal oscillations of the layered crystal are arranged in pairs; in GaSe, for example, the upper series corresponds to totally symmetric vibrations, while the vectors of the lower series correspond to the so-called "antisymmetric" vibrations. The frequency of a symmetric mode will not be characterized by the contribution of the interlayer forces, since the vibrations of the layers in the unit cell are not in phase; the interaction between selenium atoms located on the boundary of adjacent

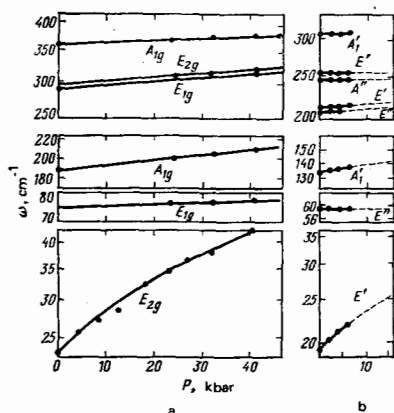


FIG. 4. Energy position of the lines in the Raman-scattering spectrum as a function of the hydrostatic pressure P at 300 K for the crystals GaS (a) and GaSe (b), according to the data of Besson.³⁵

TABLE III.

Crystal	Graphite	As_2Se_3	As_2S_3	MoS_2	GaS	GaSe
Interlayer frequency, cm ⁻¹	45	21.5 32.5	27 28	34	22	19
k_0/k_1	0.001	0.021	0.017	0.014	0.016	0.019

layers raises the frequency of an antisymmetric mode. Thus the interlayer interaction splits each normal mode into two. This splitting is analogous to the well-known Davydov splitting of the excitonic terms in a molecular crystal, which results from the intermolecular interaction of translationally inequivalent molecules in the unit cell of the crystal.³⁷ The number of components of the multiplet in the general case is determined by the number of translationally inequivalent layers. Davydov splitting cannot be detected in the Raman spectra of crystals having a center of inversion (As_2S_3 , As_2Se_3 , GaS , etc.). In this case the rule of alternative forbiddenness is in effect—there can be no vibrations which simultaneously correspond to lines in the Raman spectra and in the absorption or reflection spectra (Raman- and infrared-active modes). One of the doublet components will be observed in the infrared spectra, the other in the Raman spectra. Since the symmetry elements characterizing the ϵ structure do not include a center of inversion, both components of the doublet can be observed only in the Raman spectra. The modes forming Davydov pairs are found in the same horizontal row in Table II; in the β polytype there are 2 infrared- and 6 Raman-active vibrations. Every Raman-active vibration forms a doublet with a mode of another symmetry which is Raman-inactive. The E_{2g}^2 mode is the lowest-frequency mode in the Raman spectrum, since it forms a Davydov doublet with the acoustic mode E_{1u}^1 . In the β polytype there are 6 infrared-active vibrations, 2 of which form Davydov doublets with acoustic vibrations and are low-frequency modes. In Raman scattering there are 11 active vibrations, 10 of which form Davydov pairs which may be unresolved in the Raman spectra because of the weak interlayer interaction. Then in the Raman spectra these vibrations appear in the form of 6 lines, just as in the β polytype, and this circumstance makes it difficult to identify the polytype on the basis of the Raman-scattering data alone.

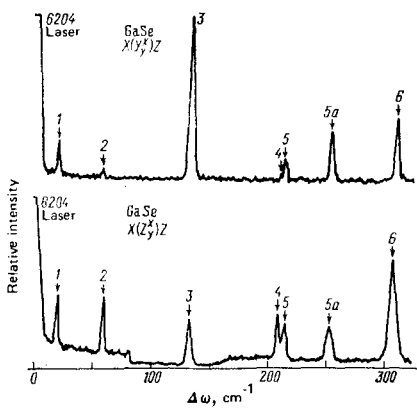


FIG. 5. Raman-scattering spectra of gallium selenide recorded at 77 K for two polarizations of the incident light.¹⁶⁷ The letters before and after the parentheses give the direction of propagation of the incident and scattered light, respectively. The letters inside the parentheses give the direction of the electric-field vector of the incident and scattered light (the z axis is directed along the optic C axis, perpendicular to the crystal layers).

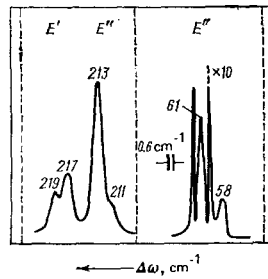


FIG. 6. Davydov splitting of several lines in the Raman spectra of ϵ -GaSe at $T=80$ K, according to the data of Artamonov *et al.*³⁸ Nicklov *et al.*²⁵ have reported the detection of a splitting of the line at $\omega=136$ cm^{-1} (the symmetry of the corresponding mode is A'^1).

In the ϵ polytype, however, there are vibrations which are simultaneously infrared- and Raman-active (E'^3 , E'^4 , and E'^2), and the Raman spectrum should contain additional lines of the indicated vibrations, corresponding to longitudinal LO modes. Figure 5 shows typical Raman-scattering spectra for GaSe crystals as recorded in an "at an angle" scattering geometry. In addition to the typical six lines (1–6), there is another noticeable line (5a), which is interpreted as an LO mode (E'^4 ; see Table II). The polarization properties of this line are consistent with such an assertion. The splitting of the lines in the Raman spectrum is not seen in Fig. 5. As a rule, special studies are required to detect this splitting. The experimentally detected splitting of a number of lines in the Raman spectrum of gallium selenide is illustrated in Fig. 6. The readily apparent (see Fig. 6) intensity difference in the components of the doublet can be explained by analogy with molecular crystals. The intensity of each component of a Davydov doublet in the exciton spectra of these crystals is determined by the sum or difference of the intramolecular dipole moments (of the two molecules in the unit cell). Since in the ϵ polytype the spatial distributions of molecules/layers having identical internal structures are not very different, the doublet component determined by the difference of the moments can turn out to be extremely small.³⁸

The existence of splitting of the phonon modes in layered semiconductors is consistent with the results of slow-neutron inelastic-scattering studies in GaS and GaSe.^{39,40} These experiments yielded data on the phonon dispersion in GaS and GaSe for the directions $\Gamma - \Delta - A$ and $\Gamma - \Sigma - M$ of the hexagonal Brillouin zone in Figs. 7 and 8. The $\Gamma - \Delta - A$ direction corresponds to

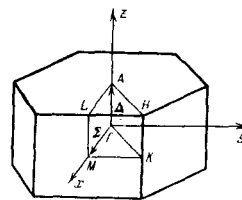


FIG. 7. First Brillouin zone for hexagonal lattice. The notation for the high-symmetry points is that of Herring.¹⁷⁰

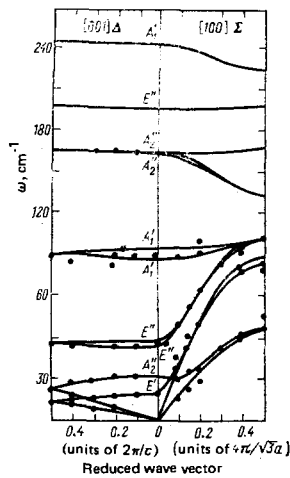


FIG. 8. Phonon dispersion in ϵ -GaSe (after Jandle *et al.*³⁹). The experimental points correspond to the data of slow-neutron inelastic-scattering studies in ϵ -GaSe, the solid lines give the phonon spectrum in GaSe as calculated with the model of the force constants described in Ref. 39.

motion at right angles to the crystal layers along the hexagonal C axis. The results of neutron-scattering experiments are, on the whole, in agreement with the frequency values of the long-wavelength phonons determined by optical methods, and also with the experimental data on the propagation velocities v_l and v_t of longitudinal and transverse sound waves, respectively, in GaSe and GaS.⁴¹

The phonon dispersion curves in GaS and GaSe are of the same character as those of graphite²⁵ and MoS₂.⁴² In the propagation of vibrations across the crystal layers all the high-frequency (intralayer) branches have an extremely small width—a weak dispersion—when the vibration propagates at right angles to the layer, whereas the frequencies of the interlayer vibrations display a substantial dependence on the wave vector for motion in any other direction. A typical circumstance is that the low-frequency optical branches (E_{2g}^2 , for example) intersect an acoustic branch. A symmetry-allowed interaction of the optical and long-wavelength acoustic vibrations in the crystal can occur. This circumstance can prove important in analyzing phenomena in which the phonon-phonon interaction plays a large role (thermal expansion, acoustic absorption, thermal resistivity). The experimental data of Jandle, Brebner and Powell^{39,40} correspond to the presently available results on the vibrational spectra of layered crystals of the III-VI group (Refs. 22, 23, 39, 40, 43, and 44) calculated with various force-constant models, the parameters of which are obtained by fitting to the known frequencies of the long-wavelength optical phonons and elastic moduli in the plane of the layer. The vibrational spectra of gallium selenide and gallium sulfide were calculated by Polian and Kunc,⁴⁵ with the long-wavelength forces taken into account in the rigid-ion model.

Using the results of their own neutron-scattering experiments, Jandle, Brebner, and Powell^{39,40} constructed the phonon dispersion curves for the principal

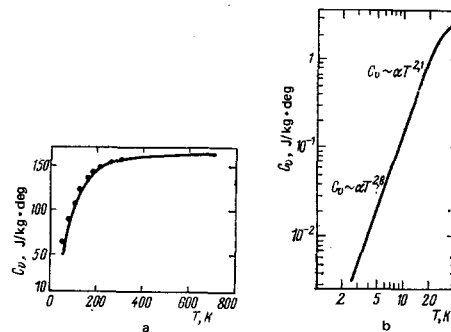


FIG. 9. a) Temperature dependence of the specific heat of gallium selenide (the points correspond to the experimental results of Mamedov *et al.*,⁴⁷ the solid curve is based on the phonon frequency distribution function $g(\omega)$ calculated by Jandle *et al.*³⁹); b) the low-temperature part of the $C_v(T)$ curve replotted in a double logarithmic scale.

directions in the Brillouin Zone, calculated the phonon frequency distribution function $g(\omega)$ for GaS and GaSe, and evaluated the specific heat C_v at various temperatures. In fact,

$$C_v = \frac{dE}{dT}, \quad E = \int_0^{\omega_0} \frac{\hbar\omega g(\omega) d\omega}{e^{\hbar\omega/kT} - 1};$$

here ω_0 is the Debye temperature and T the absolute temperature. The results of the calculations are, on the whole, in good agreement with the data from calorimetric measurements of the specific heat of gallium arsenide,⁴⁶ as can be seen in Fig. 9. The low-temperature part of the curve is shown separately in Fig. 9b.

In the temperature region $16 \leq T \leq 30$ K, the exponent α in the relation $C_v = AT^\alpha$ is equal to 2.1. The presence of a quadratic region of the function $C_v(T)$ in this temperature range is also seen in other layered semiconductors of the III-VI group.⁴⁷ At the lowest temperatures this function is of the form $C_v \sim T^3$, corresponding to the isotropic three-dimensional case, for all the crystals.

The existence of a temperature interval in which the specific heat of GaS and GaSe has a quadratic temperature dependence was interpreted by Jandle, Brebner, and Powell^{39,40} as a manifestation of the two-dimensional character of the vibrational spectra of these crystals; for the two-dimensional case $E \sim T^3$ and $C_v \sim T^2$. Since in an isotropic situation one has $C_v \sim (T/\Theta)^3$, for a two-dimensional crystal Θ should depend on T . A dependence of this sort is characteristic of graphite and, to a much smaller extent, of crystals of the GaSe type (Fig. 10).⁴⁹ An attempt can be made⁴⁶ to explain the

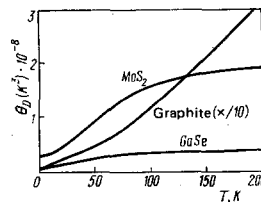


FIG. 10. Temperature dependence of the quantity θ_D^3 for several layered crystals, calculated with a model of the force constants. The parameters of the model were determined from the neutron-scattering data.⁴⁹

presence of a quadratic region on the $C_v(T)$ curve for group III–VI crystals on the basis of bending oscillations, which can occur in a crystal consisting of weakly interacting layers.⁸ An acoustic bending wave is characterized by the specific dispersion relation $\omega \sim k^2$, which, according to calculations, leads to a quadratic temperature dependence of the specific heat in a certain intermediate temperature region in which the interaction between the layers cannot be neglected.⁸

According to the results of neutron-scattering studies in graphite and MoS_2 , for transverse acoustic modes propagating in the basal plane of the layer and polarized in such a way that the electric-field vector is perpendicular to the layers (TA_1), the dispersion relation is nearly quadratic.¹⁹ Of the crystals of the III–VI group, whose layers have a more complex structure (see Fig. 1), only in GaS have acoustic waves with a quadratic wave-vector dependence of the frequency been detected experimentally.

The excitation of bending oscillations can lead to a specific temperature dependence of the linear expansion coefficient α_{\parallel} of the crystal in the plane parallel to the layers. In the temperature region in which bending waves are excited, α_{\parallel} can take on negative values. This “membrane” effect is due to the fact that the excitation of bending waves decreases the dimensions of the crystal in the plane of the layers.⁴⁸ Such a behavior of α_{\parallel} had been detected earlier in graphite. A subsequent study by G. L. Belen’kii, A. V. Solodukhin, and R. A. Suleimanov showed that α_{\parallel} assumes negative values in GaS as well, though in a much narrower temperature range than in graphite (Fig. 11). It should be noted that the existence of a temperature region in which the coefficient of linear expansion of the crystal takes on negative values and the presence of a quadratic region on the $C_v(T)$ curve in the same temperature range are evidence that bending oscillations contribute substantially to the free energy of the crystal in the given temperature range.

We have discussed the properties of the vibrational spectra of layered group III–VI crystals on the basis of the results of studies on GaS, GaSe, and InSe. The information on the phonon spectra of gallium telluride^{50–52} is less complete; the experimental studies in GaTe have been devoted primarily to determining the frequencies of the long-wavelength phonons in this crystal.

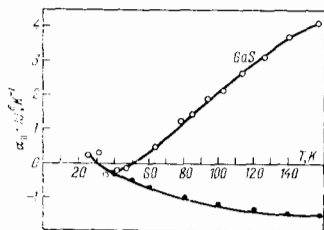


FIG. 11. Temperature dependence of the coefficient of linear expansion $\alpha_{\parallel}(T)$ of graphite and gallium sulfide in the plane parallel to the layers. The accuracy of the measurements of α is $\Delta\alpha \approx 1 \cdot 10^{-7} \text{ K}^{-1}$. The values of α_{\parallel} for graphite are those of Bailey and Yates.¹⁷¹

However, the basic features of the phonon spectra of GaS, GaSe, and InSe enumerated above share the same general character with all III–VI layered semiconductors.

4. EFFECT OF LATTICE ANISOTROPY ON THE EXCITON STATES IN LAYERED CRYSTALS

Our main goal in this review, as we mentioned in the introduction, is to explain, for the illustrative case of III–VI crystals, how the rather strong anisotropy of the chemical bonding in layered compounds affects their electronic and vibrational spectra. In the previous section we showed that all the possible modes of oscillation in layered crystals can be divided into two types: intralayer modes and the relatively low-frequency interlayer modes, which correspond to a displacement of the entire layers, acting as rigid molecules, with respect to one another. The interlayer modes arise only in the case where the unit cell contains two or more layers. All the high-frequency intralayer branches have a weak dispersion when the oscillations are propagating at right angles to the layers, e.g., in the Γ – Δ – A direction (see Fig. 7), and the weak interlayer interaction leads to a Davydov splitting of these normal modes.

The enumerated features of the vibrational spectra of layered crystals stand as evidence that the phonon subsystem in these compounds can be described in a completely satisfactory manner in terms of the quasi-two-dimensional model. It is just this circumstance that has occasioned the enormous interest in the study of the electronic properties of layered crystals, since systems with extremely anisotropic electronic properties have opened up wide possibilities for solving a number of problems in solid-state physics.^{53,54}

The assumption that the electronic subsystem in layered semiconductors is extremely anisotropic at first glance seems entirely justified. In the majority of layered crystals the metal atoms are located within the layer (see Fig. 1) and the overlap of the wave functions between adjacent layers is insignificant. Consequently, if some of the electron bands are made up of the atomic orbitals of the metal, then these bands should be quasi-two-dimensional. From this point of view dichalcogenides of transition metals, i.e., layered crystals of the types IV–VI₂ (TiS_2 , TiSe_2 , TiTe_2 , ZrS_2 , ZrSe_2 , ZrTe_2 , HfS_2 , HfSe_2 , HfTe_2), V–VI₂ (compounds of V, Nb, and Ta with S, Se, and Te), and VI–VI₂ (compounds of Mo and W with S, Se, and Te) are of the greatest interest, since in the transition elements the inner d levels are not all filled, and the d bands formed from these states are, as a rule, rather narrow, implying that the wave functions of neighboring atoms overlap only slightly. In particular, the data of Wilson and Yoffe⁵⁵ imply that in VI–VI₂ compounds the d_{z^2} band is a valence band, and the wave functions corresponding to this band can be considered localized in the layer.⁵⁶

We shall show in Sect. 6 that certain bands in GaSe crystals are also extremely anisotropic. In GaSe, however, the p_x orbitals of Se contribute significantly to the formation of the conduction and valence bands,¹¹ and

therefore the basic electronic properties of this material are practically isotropic. This conclusion is supported by numerous experiments on the electrical conductivity and optical spectra near the fundamental absorption edge. It should be noted that optical studies in the region of an interband absorption threshold, where the optical properties in the case of allowed direct transitions are determined to a large degree by excitonic effects, are among the most informative methods. However, before turning to an analysis of the results of the main experimental studies of the optical properties of compounds of this group, we think it is important to consider the question of how the energy spectrum and wave functions of a free exciton are affected by the existence of anisotropy in layered semiconductors. Here we shall not take into account the exchange interaction (which leads to a complex structure of the ground state), scattering processes due to the exciton-phonon interaction, polariton effects, etc. In this case to determine the energy spectrum and wave functions of an exciton in the effective-mass approximation one must solve the Schrödinger equation for a uniaxial crystal⁵⁷

$$\left\{ -\frac{\hbar^2}{2\mu_{\perp}} \left(\frac{\partial^2}{\partial x^2} + \frac{\partial^2}{\partial y^2} \right) - \frac{\hbar^2}{2\mu_{\parallel}} \frac{\partial^2}{\partial z^2} - \frac{e^2}{[\epsilon_{\parallel} \epsilon_{\perp} (x^2 + y^2) + \epsilon_{\parallel}^2 z^2]^{1/2}} - E \right\} F(r) = 0, \quad (1)$$

where

$$\frac{1}{\mu_{\perp}} = \frac{1}{m_{\perp}^e} + \frac{1}{m_{\perp}^h}, \quad \frac{1}{\mu_{\parallel}} = \frac{1}{m_{\parallel}^e} + \frac{1}{m_{\parallel}^h},$$

the z axis is chosen in the direction of the optic C axis of the crystal, and the subscripts \parallel and \perp indicate that the corresponding values of the mass m or dielectric constant ϵ are taken either in the direction of the C axis or perpendicular to it.

The exciton wave function is

$$\Psi_{v,c}(r_e, r_h) = F(r_e - r_h) \varphi_v(k_0, r_h) \varphi_c(k_0, r_e), \quad (2)$$

where φ_v and φ_c are the Bloch wave functions in the valence and conduction bands at the critical point k_0 . The function $F(r_e - r_h)$ is the solution of equation (1). Equation (1) is also valid for solving the problem of the energy spectrum of shallow donors in semiconductors of the germanium and silicon type, in which the critical point k_0 for the electron band is not located at the center of the Brillouin zone, and the constant-energy surfaces are ellipsoids of revolution (in this case $\epsilon_{\perp} = \epsilon_{\parallel} = \epsilon_0$, while $\mu_{\perp} = m_{\perp}^e$, $\mu_{\parallel} = m_{\parallel}^e$). Therefore, we shall also discuss some results of donor-level calculations in Ge and Si.

Equation (1) is usually transformed to:

$$\left(\nabla^2 + \frac{2}{\sqrt{x^2 + y^2 + \gamma z^2}} + E \right) F(r) = 0, \quad (3)$$

where $\gamma = \epsilon_{\perp} \mu_{\perp} / \epsilon_{\parallel} \mu_{\parallel}$ (for the problem of donors in Ge and Si $\gamma = m_{\perp}^e / m_{\parallel}^e$), and the energy and length, respectively, are measured in units of the effective excitonic rydberg $Ry^* = \mu_{\perp} e^4 / 2\hbar^2 \epsilon_{\perp} \epsilon_{\parallel}$ and the exciton Bohr radius $a_0^* = \hbar^2 \sqrt{\epsilon_{\perp} \epsilon_{\parallel}} / \mu_{\perp} e^2$. Equation (3) is obtained from (1) by the change of variables: $x' = x$, $y' = y$, $z' = \sqrt{\mu_{\parallel} / \mu_{\perp}} z$ (the primes will from now on be dropped from the new variables). If $\gamma = 1$ the energy spectrum is purely hydro-

genic: $E_n = n^{-2}$. However, since we have made a change of variables, the wave functions and the exciton Bohr radius a_0^* can be highly anisotropic, for the anisotropy of the reduced masses of the exciton can be compensated by the anisotropy of the dielectric constant.

Let us now consider the case of maximum anisotropy, $\gamma = 0$. The solution of the corresponding Schrödinger equation for $E < 0$ (the energy is measured from the bottom of the conduction band) is

$$E_n = -\frac{1}{(n+1/2)^2}, \quad n=0, 1, 2, \dots, \quad (4)$$

$$F_{nm}(r) = \left[\frac{(n-|m|)!}{\pi a_0^{*2} (n+1/2)^2 (n+|m|)!^2} \right]^{1/2} e^{-\frac{1}{2} \rho} \rho^{|m|} L_{n-|m|}^{2|m|}(\rho) e^{im\varphi}, \quad (5)$$

where $\rho = r/a_0^* \lambda$, $\lambda^{-2} = -4E/Ry^*$, and the $L(\rho)$ are Laguerre polynomials.^{58, 61} Each energy level is degenerate with respect to the magnetic quantum number m (the multiplicity of the degeneracy is $2n+1$) and with respect to the coordinate z , which in this case plays the role of a continuously variable quantum number.

In comparing the energy spectrum of an extremely anisotropic exciton with the usual hydrogen-like spectrum, one should keep in mind that the two-dimensional exciton is much more stable. In addition, the excited states of such an exciton are considerably farther from the ground state than in the three-dimensional case. If, for example, it is assumed that the ground states coincide, i.e., the binding energies of the two- and three-dimensional excitons are the same, then the first excited state of the two-dimensional exciton ($n=1$) will coincide with the second excited state of the three-dimensional exciton ($n=3$), the second with the fourth, and so on. This circumstance makes it somewhat difficult to detect experimentally the exciton series of the type in (4), since in real crystals the presence of broadening due to various scattering mechanisms can make it impossible to observe a sufficient number of terms in the series. For example, Beal *et al.*⁶² studied the transmission spectra of the 2H and 3R modifications of MoS₂ at 5 K. It is known⁶³ that the exciton binding energies in crystals of these two modifications are nearly the same. However, in spite of the fact that the half-width of the absorption line of the excitonic ground state in 3R-MoS₂ is half as large as in a crystal of the 2H polytype, excited states are not seen in the spectrum, in contrast to the case of 2H-MoS₂. This circumstance admits the conjecture⁶⁵ that the excitons in 3R-MoS₂ are extremely anisotropic; this conjecture no doubt requires further verification on more perfect samples.

The presence of excitonic effects, i.e., allowance for the Coulomb interaction of the electron and hole, not only leads to the appearance of discrete levels in the band gap but also alters the absorption coefficient somewhat at $\hbar\omega \approx E_g$, where E_g is the width of the band gap. The contribution of excitonic effects to the absorption for photon energies $\hbar\omega \approx E_g$ is usually taken into account by the so-called Sommerfeld factor, which is maximum for $\hbar\omega \sim E_g$ and decreases markedly with increasing energy. In the three-dimensional case allowance for the Sommerfeld factor does not lead to any kind of features in the frequency dependence of the ab-

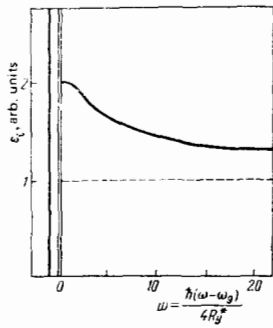


FIG. 12. Energy dependence of the imaginary part ϵ_i of the dielectric permittivity near the critical point corresponding to the two-dimensional minimum, with allowance for excitonic effects.

sorption coefficient. In the case of extreme anisotropy the situation is essentially different. Taking into account that the density of states in the two-dimensional case for $E > E_g$ is independent of the energy E , the frequency dependence of the absorption coefficient for allowed direct transitions, when the matrix element of the transition is also energy independent, should be of the form of a rectangular step,⁶⁰ in contrast to the square root threshold in the three-dimensional case. Therefore, the contribution of excitonic absorption in this region of the spectrum can lead to the appearance of a maximum ("hump") near $\hbar\omega \approx E_g$.

Figure 12 shows the frequency dependence of the imaginary part ϵ_i of the dielectric function at a critical point of the type M_0 (an absolute minimum, i.e., the fundamental absorption edge) for the two-dimensional problem.⁵⁹

The absorption coefficients of layered crystals with extremely anisotropic electronic properties were calculated for various regions of the spectrum by Shinada and Sugano.⁶¹ Table IV gives the results of these calculations for allowed direct transitions, and also the corresponding functions in the isotropic case. No features of the "hump" type arise in the spectral dependence of the absorption coefficient for forbidden direct transitions.⁶¹ An analogous situation evidently should also occur for any other type of interband optical transi-

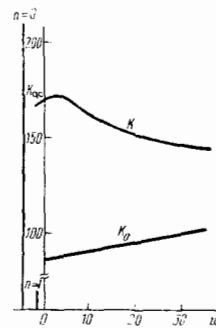


FIG. 13. Spectral dependence of the absorption coefficient K of GaSe layered crystals ($Ry = 12.5$ meV, $E_g = \hbar\omega_g = 2.11$ eV) in the case of an extremely anisotropic subsystem. Here K_{qc} is the absorption coefficient in the region of the quasi-continuum of exciton states and K_0 is the absorption coefficient without allowance for excitonic effect.⁶¹

tions, so that the allowed direct transitions in two-dimensional systems have a special status in this regard.

Figure 13 shows the frequency curves of the absorption coefficient for layered GaSe crystals in the region of the quasi-continuum of exciton states (K_{qc}) and in the continuum both with (K) and without (K_0) allowance for excitonic effects, under the assumption that the electronic properties of this compound are extremely anisotropic. Here the excitonic rydberg was assumed to be $Ry \sim 12.5$ meV, and $E_g = 2.11$ eV. In addition, the matrix element of the transition between the valence (v) and conduction (c) bands under the action of electromagnetic radiation with a polarization vector e and frequency ω was assumed to depend linearly on the frequency of the light. The linear rise of K_0 in Fig. 13, in contrast to the results of Velicky and Sak⁵⁹ and Ralph,⁶⁰ is explained precisely by the dependence of the transition matrix element on ω . We note that for allowed direct transitions the transition probability is by definition independent of the frequency ω of the electromagnetic radiation. Nevertheless, the results (shown in Fig. 13) of calculations of the spectral dependence of the absorption coefficient can apparently be used (with allowance for the initial assumptions) for GaSe crystals, in which for the geometry $e \perp c$ the functional form of the transi-

TABLE IV.

	Two-dimensional case	Three-dimensional case
f_n	$\frac{2}{\pi m_0 (a_0^*)^2 \hbar \omega} \left(n + \frac{1}{2}\right)^{-3} \langle c \mathbf{e} \mathbf{p} v \rangle ^2$ $n = 0, 1, 2, \dots$	$\frac{2}{\pi m_0 (a_0^*)^3} n^{-3} \langle c \mathbf{e} \mathbf{p} v \rangle ^2, n = 1, 2, 3, \dots$
k_{qc}	$\frac{8\pi \sqrt{\epsilon_{\perp} \epsilon_{\parallel}}}{m_0^2 c n_r (a_0^*)^2 \omega} \langle c \mathbf{e} \mathbf{p} v \rangle ^2$	$\frac{8\pi \epsilon_0}{m_0^2 c n_r (a_0^*)^2 \omega} \langle c \mathbf{e}, \mathbf{p} v \rangle ^2$
k	$\frac{k_0 e^{\pi (a_0^* k)^{-1}}}{\cos \hbar \pi (a_0^* k)^{-1}}$	$\frac{k_0 \pi (a_0^* k)^{-1} e^{\pi (a_0^* k)^{-1}}}{\sin \hbar \pi (a_0^* k)^{-1}}$
k_0	$\frac{4\pi \sqrt{\epsilon_{\perp} \epsilon_{\parallel}}}{m_0^2 c n_r (a_0^*)^2 \omega} \langle c \mathbf{e} \mathbf{p} v \rangle ^2$	$\frac{4}{m_0^2 c n_r (a_0^*)^2 \omega} \sqrt{\frac{\hbar \omega - E_g}{Ry}} \times \langle c \mathbf{e}, \mathbf{p} v \rangle ^2$

f_n is the oscillator strength for the optical transitions to the exciton states with principal quantum number n ; n_r is the real part of the refractive index; $a_0^* = \hbar^2 \sqrt{\epsilon_{\perp} \epsilon_{\parallel}} / e^2 \mu_1$ is the effective Bohr radius, and $Ry^* = \mu_1 e^4 / 2 \hbar^2 \epsilon_{\perp} \epsilon_{\parallel}$ is the effective excitonic rydberg.

tion matrix element is suitable for the given calculations in the region of small wave vectors k .⁶⁴

Thus the presence of a "hump" on the frequency dependence of the absorption coefficient for allowed direct transitions could serve as proof of the quasi-two-dimensionality of the excitons in layered semiconductors. However this proof should not be regarded as unambiguous, since similar "humps" have been observed in the absorption spectra of GaSe and GaTe^{65, 66} in spite of the three-dimensional character of the excitons in GaSe (see Sect. 5). Therefore, the chief criterion for the quasi-two-dimensionality of the excitons must be an energy spectrum of the type in (4).

As we have already mentioned, systems with extremely anisotropic electronic properties are of great interest for solid-state physics. Unfortunately, there are as yet no unambiguous demonstrations of the existence of such systems among the layered crystals that have been studied. As a rule, in layered semiconductors for which there are enough experimental data that one can determine the anisotropy parameter $\gamma = \epsilon_{\perp} \mu_{\perp} / \epsilon_{\parallel} \mu_{\parallel}$, the value of γ turns out to be not much different from unity for the bands which govern the basic properties, i.e., for the conduction and valence bands. Nevertheless, these basic properties are substantially different from those which are found in isotropic crystals. We have already noted that even for $\gamma = 1$ the exciton wave functions and Bohr radius in layered crystals can be anisotropic. For $\gamma \neq 1$ the exciton energy spectrum should also change, since the anisotropy lifts the degeneracy with respect to the orbital quantum number l that is characteristic for a Coulomb center. Since the Hamiltonian in equations (1) and (3) has axial symmetry, its eigenfunctions are characterized by a magnetic quantum number $m_z = m$ and a parity P (Ref. 67).

Equations (1) and (3) have been solved by many authors.⁶⁸⁻⁸¹ All the papers cited can be arbitrarily divided into two groups. The first group includes the papers in which the solution of (1) and (3) is found with the aid of perturbation theory (Refs. 69-71, 73, 74, 77, and 79). It is only natural that these solutions have a significantly lower accuracy than the results of variational calculations (the second group of papers, Refs. 68, 72, 75, 76, and 80), especially in the region of rather high anisotropy. Figure 14 shows the results of various authors^{80, 81} for the calculated ground-state energy as a function of the anisotropy parameter γ . The best results on the ground-state energy are obtained by a direct variational method with a trial function of the form

$$f = (\pi a_{\perp}^2 a_{\parallel})^{-1/2} \exp \left\{ - \left(\frac{\rho^2}{a_{\perp}^2} + \frac{z^2}{a_{\parallel}^2} \right)^{1/2} \right\}, \quad (6)$$

where $\rho^2 = x^2 + y^2$, and a_{\perp} and a_{\parallel} are variational parameters.^{68, 80} Function (6) is essentially the product of the exact solutions of the two- and three-dimensional Schrödinger equations. Somewhat poorer results are obtained when a linear combination of hydrogen-like orbitals are used as trial functions.^{72, 75} Even if one uses⁷⁵ the 42 wave functions describing the lowest states of the same parity with $m = 0$, i.e., all the way to $n = 12$, the calculation is only good in the interval from

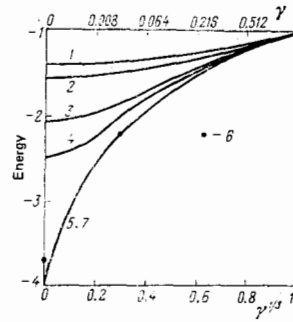


FIG. 14. Dependence of Λ_c/m^2 and Λ_b/m^2 on the relative saturation magnetization m for the alloy $Tb_{0.5}Gd_{0.5}$. $\gamma = \epsilon_{\perp} \mu_{\perp} / \epsilon_{\parallel} \mu_{\parallel}$ (for donors $\gamma = m_1^e / m_n^e$): 1) Ref. 70, 2) Ref. 69, 3) Ref. 73, 4) Ref. 78, 5) Ref. 80, 6) Ref. 68, 7) Ref. 72. In Ref. 72 calculations were carried out for a range of $\gamma = m_1^e / m_n^e$ from 1 to 10^{-3} . The energy is in units of $Ry^* = \mu_{\perp} e^4 / 2\hbar^2 \epsilon_{\perp} \epsilon_{\parallel}$ (for donors $Ry = m_1^e e^4 / 2\hbar^2 \epsilon^2$).

$\gamma = 1$ to $\gamma = 0.2$. This circumstance is due mainly to certain difficulties of a purely computational nature which arise for this choice of trial functions. If these difficulties are overcome, the results obtained in this way have a rather high accuracy.⁷²

For variational calculations of the energy of the excited states of the excitons in layered crystals or of the donors in Ge and Si, the trial functions given in Table V are used.^{67, 68}

Figure 15 shows the calculated results⁷² for the energies of the s -like donor levels as a function of the anisotropy parameter $\gamma = m_1^e / m_n^e$.

A rather interesting question arises in regard to the problem of the excited states—namely, to what limit should the energy of some level or other tend as $\gamma \rightarrow 0$? A partial answer to this question is found in Fig. 16, which shows the energies of the $1s$, $2p_0$, $2s$, and $2p_{\pm}$ excitonic states as functions of the anisotropy parameter γ .⁸¹ It is clear from the most general considerations that, as a consequence of the axial symmetry of the Hamiltonian of an anisotropic exciton, the eigenfunctions with a given m and parity P are superpositions of the Coulomb-center states (the three-dimensional case) with different n but with the given m and P . For example,⁶⁷ the wave function with $m = 0$ and positive parity is a superposition of the $1s$, $2s$, $3s$, $3d$, $4s$, $4d$, etc. states with $m = 0$. Therefore, all these states should have the limit -4 at $\gamma \rightarrow 0$. An analogous con-

TABLE V.

State	Trial function
$1s$	$c \exp \left[- \left(\frac{\rho^2}{a^2} + \frac{z^2}{b^2} \right)^{1/2} \right]$
$2p_0$	$cz \exp \left[- \left(\frac{\rho^2}{a^2} + \frac{z^2}{b^2} \right)^{1/2} \right]$
$2s$	$(c_1 + c_2 \rho^2 + c_3 z^2) \exp \left[- \left(\frac{\rho^2}{a^2} + \frac{z^2}{b^2} \right)^{1/2} \right]$
$2p_{\pm}$	$cx \exp \left[- \left(\frac{\rho^2}{a^2} + \frac{z^2}{b^2} \right)^{1/2} \right]$
$3p_0$	$(c_1 + c_2 \rho^2 + c_3 z^2) z \exp \left[- \left(\frac{\rho^2}{a^2} + \frac{z^2}{b^2} \right)^{1/2} \right]$

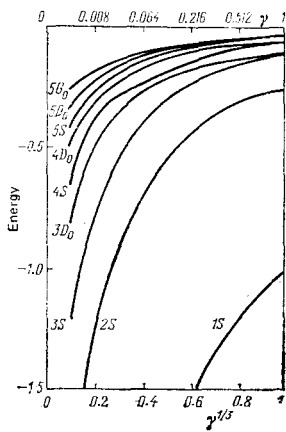


FIG. 15. Energy of s-like donor levels versus the anisotropy parameter $\gamma = m_1^e/m_{H1}^e$, according to the data of Daulkner.⁷² The energy unit is $m_1 e^4/2\hbar^2\epsilon^2$.

clusion was reached by Gerlach and Pollman⁸¹ using the theorem of McDonald.⁸² Since the sequence of levels for $\gamma \approx 1$ is known exactly and, by virtue of McDonald's theorem, levels with fixed m and parity P cannot cross, all these levels have the same limit for $\gamma \rightarrow 0$.

Of the papers in which equations (1) and (3) are solved by perturbation theory, those of Pollman and Gerlach⁷⁷⁻⁷⁹ enjoy a special status. The results of those papers, as can be seen in Fig. 14, are closest to those of the variational calculations.^{72,80} If one adopts the results of Refs. 72 and 80 as exact solutions, then the estimates of Gerlach and Pollman⁷⁸ show that their solution is almost exact in the range $\gamma = 1-0.8$, and in the range $\gamma = 0.8-0.6$ the error does not exceed 5%.

It should be noted that, in contrast to the variational calculations, perturbation-theory calculations can give the solution of the initial Schrodinger equation (1), (3) in analytical form, which is a definite convenience for comparing theory and experiment. Since we shall later use the results of Refs. 77-79 (these being the most ex-

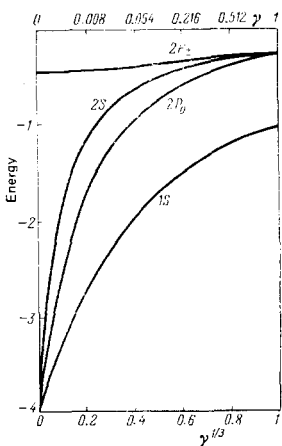


FIG. 16. Energy of 1s, 2p₀, 2s, and 2p states of the exciton versus the anisotropy parameter $\gamma = \epsilon_1 \mu_1 / \epsilon_{H1} \mu_{H1}$, as given by McDonald.⁸² The energy unit is $Ry^* = \mu_1 e^4/2\hbar^2\epsilon_1\epsilon_{H1}$.

act of the perturbation-theory results) to determine the anisotropy parameter γ in GaSe crystals, let us examine these results in more detail.

In Ref. 77, Pollman proposed a certain refined self-consistent version of perturbation theory which proved extremely efficient for solving equation (3). Let the initial Hamiltonian be

$$H = H_0 + H_p = T + V_0 + H_p \quad (7)$$

and let ψ_0 and E_0 be the exact solution of the unperturbed problem. We write the perturbation in the form of a product of V_0 and V_p :

$$H_p = V_0 V_p. \quad (8)$$

Then

$$H = T + V_0(1 + \langle \psi_0 | V_p | \psi_0 \rangle) + V_0(V_p - \langle \psi_0 | V_p | \psi_0 \rangle) = H_0^1 + H_p^1, \quad (9)$$

where $H_0^1 = T + \lambda V_0$, with $\lambda = 1 + \langle \psi_0 | V_p | \psi_0 \rangle$. Since the equation $H_0 \psi_0 = E_0 \psi_0$ is solved exactly, the equation $H_0^1 \psi_0^1 = E_0 \psi_0^1$ is also solved exactly. The functions ψ_0^1 can therefore be used for the subsequent averaging of $V_p^1 = V_p - \langle \psi_0 | V_p | \psi_0 \rangle$, etc. As a result of ν approximations one obtains a function ψ_0^ν which is almost equal to the function $\psi_0^{\nu-1}$, and the initial Hamiltonian is

$$H = T + V_0(1 + \langle \psi_0^\nu | V_p^\nu | \psi_0^\nu \rangle) + V_0(V_p^\nu - \langle \psi_0^\nu | V_p^\nu | \psi_0^\nu \rangle) = H_0^{\nu+1} + H_p^{\nu+1}. \quad (10)$$

Applying the above procedure to equation (3), we obtain⁷⁶

$$H = \nabla_r^2 + \frac{2}{(x^2 + y^2 + z^2)^{1/2}} = \nabla_r^2 + \frac{2}{r} \frac{1}{\sqrt{1 - \alpha \cos^2 \theta}} = \nabla_r^2 + \frac{2}{r} f(\alpha, \theta), \quad (11)$$

where $\alpha = 1 - \gamma$. The solution of the unperturbed problem ($\gamma = 1, \alpha = 0$) is well known:

$$F_{nlm} = R_{nl}(r) Y_{lm}(\theta, \varphi). \quad (12)$$

Then the Hamiltonian (11) is written in the following way:

$$H = \nabla_r^2 + \frac{2}{r} Z_{lm}(\alpha) - \frac{2}{r} [Z_{lm}(\alpha) - f(\alpha, \theta)] = H_0^{lm} + H_p^{lm}, \quad (13)$$

where

$$Z_{lm}(\alpha) = \langle Y_{lm} | f(\alpha, \theta) | Y_{lm} \rangle_{\Omega}. \quad (14)$$

The quantity $Z_{lm}(\alpha)$ has the meaning of an effective charge due to the presence of anisotropy. Therefore, the solution of the Schrödinger equation in zeroth order differs from the solution in the isotropic case ($\alpha = 0$). These solutions, as we have mentioned, are rather exact at small values of α , since the correction to the energy in the first order of perturbation theory vanishes,⁷⁷ and the subsequent corrections are rather small. For analyzing the experimental data we shall use the solutions in zeroth order, which are of the form

$$F_{(nl)m}(\mathbf{r}, \alpha) = R_{nl}[Z_{lm}(\alpha), \mathbf{r}] Y_{lm}(\theta, \varphi), \quad (15)$$

$$E_{(nl)m}(\alpha) = -\frac{1}{n^2} Z_{llm}(\alpha).$$

It follows from (15) that, first, for values of α that are not too large (say, $\alpha < 0.5$, or $\gamma = 1-0.5$) the energy spectrum for fixed values of l and m remains hydrogen-like at $\alpha \neq 0$ with, of course, an excitonic rydberg that varies as a function of the anisotropy owing to the introduction of the effective charge $Z_{lm}(\alpha)$; second, since $Z_{lm}(\alpha) \neq Z_{l'm'}(\alpha)$ for $l \neq l'$ and $|m| \neq |m'|$, the de-

TABLE VI.

State	Effective charge	Dependence on anisotropy
s	$Z_{00}(\alpha)$	$I_1(\alpha)$
p_0	$Z_{10}(\alpha)$	$\frac{3}{2} \left[\frac{1}{\alpha} I_1(\alpha) - I_2(\alpha) \right]$
$p_{\pm 1}$	$Z_{1\pm 1}(\alpha)$	$\frac{3}{2} \left[\left(1 - \frac{1}{2\alpha}\right) I_1(\alpha) + \frac{1}{2} I_2(\alpha) \right]$
d_0	$Z_{20}(\alpha)$	$\frac{5}{4} \left[\left(\frac{27}{8\alpha^2} - \frac{3}{\alpha} + 1 \right) I_1(\alpha) + \frac{3}{4} \left(1 - \frac{9}{2\alpha}\right) I_2(\alpha) \right]$
$d_{\pm 1}$	$Z_{2\pm 1}(\alpha)$	$\frac{15}{4} \left[\left(\frac{1}{\alpha} - \frac{3}{4\alpha^2} \right) I_1(\alpha) - \frac{1}{2} \left(1 - \frac{3}{2\alpha}\right) I_2(\alpha) \right]$
$d_{\pm 2}$	$Z_{2\pm 2}(\alpha)$	$\frac{15}{8} \left[\left(1 - \frac{1}{\alpha} + \frac{3}{8\alpha^2}\right) I_1(\alpha) + \frac{3}{4} \left(1 - \frac{1}{2\alpha}\right) I_2(\alpha) \right]$
		$I_1(\alpha) = \begin{cases} \frac{1}{\sqrt{\alpha}} \arcsin \sqrt{\alpha} & \alpha > 0, \\ 1, & \alpha = 0, \\ \frac{1}{\sqrt{ \alpha }} \operatorname{Arsh} \sqrt{ \alpha } & \alpha < 0. \end{cases} \quad I_2(\alpha) = \frac{\sqrt{1-\alpha}}{\alpha},$

generacy with respect to quantum numbers l and m that is characteristic of a Coulomb center is lifted in the presence of anisotropy.

Pollman⁷⁷ obtained analytical expressions for the effective charge $Z_{lm}(\alpha)$ as a function of the anisotropy $\alpha = 1 - \gamma$ on the basis of relation (14)

$$Z_{lm}(\alpha) = \int_0^\pi d\theta \frac{[Y_{lm}(\theta)]^2}{[1 - \alpha \cos^2 \theta]^{1/2}}. \quad (16)$$

These expressions are given in Table VI for the first six different functions $Z_{lm}(\alpha)$, which describe the behavior of all the s, p, and d quantum states for all possible values of the principal quantum number n .

5. ANISOTROPY OF EXCITONS IN GALLIUM SELENIDE

Let us use the results presented in the previous section to analyze the properties of the exciton states in GaSe layered crystals. Excitons are formed in gallium selenide as a result of the Coulomb interaction of an electron in the conduction band of symmetry Γ_8 (with allowance for spin) and a hole in the valence band of symmetry Γ_7 [with allowance for the spin-orbit mixing of the valence bands $\Gamma_1(A_1^*)$ and Γ_5].^{62, 61} The excitonic ground state in GaSe is split by the exchange interaction into three terms:

$$\Gamma_8 \times \Gamma_7 = \Gamma_3 + \Gamma_4 + \Gamma_6 (A_1^* + A_2^* + E^*),$$

two of which are optically active: Γ_4 ($S=0$, singlet) and Γ_6 ($S=1$, triplet).⁸³

The exchange-induced fine structure of the excitonic ground state in GaSe and the selection rules for optical transitions have been discussed repeatedly in the literature (see, for example, the review by Mooser and Schlüter⁶⁴). We shall therefore not touch upon these questions here. We shall also omit from discussion the considerable experimental data on photoluminescence,^{84, 85} since there is still no consensus on the nature of a number of lines in the emission spectra. The difficulties of interpreting the emission spectrum of gallium selenide are largely due to the existence of an energy resonance between the bands of the direct and indirect excitons in this crystal.⁸⁶ To a certain extent

these difficulties have been overcome⁸⁷⁻⁸⁹ through the use of the technique of optically detected magnetic resonance (ODMR) in studies of the emission spectra of gallium selenide.

This section is devoted mainly to answering the question of how the extremely high anisotropy of the crystal lattice affects the excitonic states in gallium selenide. To answer this question one must use the experimental data to determine the anisotropy parameter $\gamma = \mu_{\perp} \epsilon_{\perp} / \mu_{\parallel} \epsilon_{\parallel}$ and then, using some theory or other, calculate the exciton energy spectrum and compare it with the experimental results if such are available. This program can be carried out for far from all layered crystals, and this circumstance to a large extent explains the choice of III-VI compounds and GaSe in particular as the main objects of study in this review.

In the first studies of the optical properties of layered crystals and GaSe in particular, many authors attempted to interpret their results on the basis of a quasi-two-dimensionality of the electronic subsystem inferred from the high degree of anisotropy of the crystal lattices of these compounds. This approach proved unsuccessful. It turned out that the energy spectrum of a direct exciton in GaSe, as determined from the absorption spectra,⁹⁰ is described in an entirely satisfactory manner by the expression

$$E_n = E_g - \frac{Ry}{n^2},$$

which is valid for the isotropic case.

A "hyperfine" structure has also been detected^{91, 92} in the two optically active terms of the ground state, with a maximum of ten⁹⁰ components in this "hyperfine" structure. The "hyperfine" structure has been observed not only in the luminescence spectra,^{85, 93} in the production of which exciton-impurity complexes can play a role, but also in the absorption and reflection spectra.^{64, 91}

Today it is assumed that the complex structure of the excitonic ground state is due to stacking faults in the adjacent layers, i.e., to the lack of periodicity in the

direction of the C axis of the crystal. Stacking faults are typical of layered compounds whose crystal lattices have many modifications which, owing to the weak nature of the interaction between layers, are energetically equivalent. For example, in GaSe crystals the ε and γ polytypes have almost the same value of the gap width E_g , and the band gap in β -GaSe is only 50 meV wider.⁹⁴ Real GaSe crystals, as a rule, are a mixture of the ε and γ polytypes if the temperature control, for example, is not precise enough during their growth.

In the first papers,⁹¹ where it was assumed that an exciton in GaSe is localized in a single layer because of the large hole mass m_h^h in the direction of the C axis,⁹⁵ the "hyperfine" structure was attributed to the varied environment of such an exciton. However, this model could not explain why the maximum number of components in the spectrum is ~ 10 , as is observed experimentally. One is obliged to assume that the exciton Bohr radius encompasses several layers [5 layers, since the number of combinations of 5 things taken 2 at a time (the ε and γ polytypes) is precisely equal to 10], i.e., the excitons in GaSe are practically isotropic.

Since the complex structure of the ground state is a consequence of the features of the crystal lattice of layered compounds, let us examine this question in somewhat greater detail. Figures 17 and 18 show absorption⁹⁰ and reflection⁹⁴ spectra which clearly reveal the "hyperfine" structure of the excitonic ground state in GaSe. A theoretical explanation of this effect was proposed in Refs. 96-98.

This explanation is based on the completely valid assumption that the translational invariance of the excitonic Hamiltonian in the direction of the C axis of the crystal in the effective-mass approximation is broken by stacking faults. Therefore, the Hamiltonian of the real crystal (a mixture of different polytypes) differs from the Hamiltonian H_0 of the ideal crystal by a potential $V(\mathbf{r}, \mathbf{R})$ which fluctuates rapidly with distance along the C axis:

$$H = \left(-\frac{\hbar^2}{2\mu} \nabla_{\mathbf{r}}^2 - \frac{e}{\varepsilon_0 \mathbf{r}} \right) - \frac{\hbar^2}{2M} \nabla_{\mathbf{R}}^2 + V(\mathbf{r} + \mathbf{R}) = H_0 + V(\mathbf{r}, \mathbf{R}), \quad (17)$$

where to simplify the notation we take $\mu_{\perp} = \mu_{\parallel} = \mu$, $\varepsilon_{\perp} = \varepsilon_{\parallel} = \varepsilon_0$, $M = m_e + m_h$, $\mathbf{R} = (m_e \mathbf{r}_e + m_h \mathbf{r}_h)/M$, and $\mathbf{r} = \mathbf{r}_e - \mathbf{r}_h$. The potential $V(\mathbf{r}, \mathbf{R})$ acts separately on the electrons and holes:

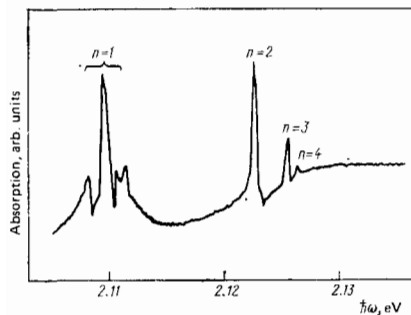


FIG. 17. Absorption spectrum of GaSe crystals in the region of direct excitonic transitions.

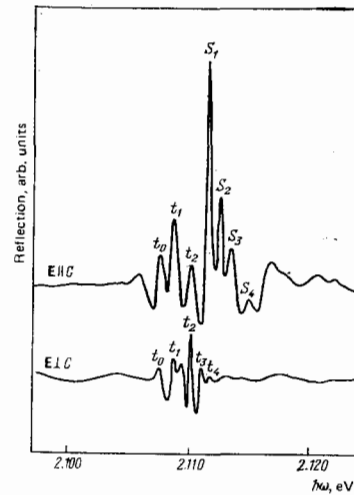


FIG. 18. Reflection spectrum of GaSe crystals plotted as a function of the incident photon energy.

$$V(\mathbf{r}, \mathbf{R}) = \delta V \left(\mathbf{R} + \frac{m_e}{M} \mathbf{r} \right) - V \delta \left(\mathbf{R} - \frac{m_h}{M} \mathbf{r} \right), \quad (18)$$

and, in essence, couples the relative motion of the electron and hole with the motion of the exciton as a whole. One seeks a solution of the Schrödinger equation with Hamiltonian (17) in the adiabatic approximation, i.e., the desired excitonic wave function $\Phi(\mathbf{r}, \mathbf{R})$ is written in the form of a product:

$$\Phi(\mathbf{r}, \mathbf{R}) = f(\mathbf{R}) \varphi(\mathbf{r}, \mathbf{R}), \quad (19)$$

where the function $\varphi(\mathbf{r}, \mathbf{R})$ is assumed to be a slowly varying function of \mathbf{R} , so that the \mathbf{R} dependence of the function $\Phi(\mathbf{r}, \mathbf{R})$ is completely determined by the function $f(\mathbf{R})$. This assumption is valid for the case in which the first and second derivatives of $\varphi(\mathbf{r}, \mathbf{R})$ with respect to \mathbf{R} can be neglected. Substituting (19) into the Schrödinger equation, we obtain

$$\left[-\frac{\hbar^2}{2\mu} \nabla_{\mathbf{r}}^2 - \frac{e^2}{\varepsilon_0 r} + V(\mathbf{r}, \mathbf{R}) \right] \varphi(\mathbf{r}, \mathbf{R}) = E(\mathbf{R}) \varphi(\mathbf{r}, \mathbf{R}), \quad (20)$$

$$\left[-\frac{\hbar^2}{2M} \nabla_{\mathbf{R}}^2 + E(\mathbf{R}) \right] f(\mathbf{R}) = \mathcal{E} f(\mathbf{R}), \quad (21)$$

The potential $E(\mathbf{R})$ in equation (21), which describes the motion of the exciton as a whole, is aperiodic in the direction of the C axis, and the excitons will therefore be localized within several layers along the axis of aperiodicity. In other words, the function $f(\mathbf{R})$ which solves equation (21) is a wave packet and not a plane wave, as for the ideal crystal, and this should also alter the selection rules on optical transitions.

Thus the presence of disorder in the sequence of alternation of the layers leads to localization of the exciton, with different forms of disorder giving different values of the energy E . The excited states will be influenced by this disorder to a much smaller degree, as can be seen from the following considerations. If we write the function $\varphi(\mathbf{r}, \mathbf{R})$ in the form

$$\varphi_n(\mathbf{r}, \mathbf{R}) = \varphi_n^0(\mathbf{r}) + \sum \frac{\langle \varphi_n^0 | V(\mathbf{r}, \mathbf{R}) | \varphi_n^0 \rangle}{E_n^0 - E_n^0} \varphi_n^*(\mathbf{r}), \quad (22)$$

where $\varphi_n^0(\mathbf{r})$ are the unperturbed hydrogen-like wave functions, we see that, since $V(\mathbf{r}, \mathbf{R})$ is a rapidly oscillating function of \mathbf{R} ,

TABLE VII.

Parameter	m_{\perp}^e/m_0	m_{\parallel}^e/m_0	m_{\perp}^h/m_0	m_{\parallel}^h/m_0	μ_{\perp}/m_0	μ_{\parallel}/m_0	γ	Reference
LCAO	0.15**)	0.36	1.67		0.14**)		0	66
EPM	0.58	0.2	1.05	0.2*)	0.37	0.1	5	11
EPM	0.12	0.51	0.6	0.4	0.1	0.22	0.61	172
LCAO-MO	0.22	0.13	-4	0.12	0.23	0.06	5.14	107
MA	0.20		0.45		0.14			173
MA					0.14	0.11	1.8	64
σ	0.17	0.3	0.8	0.2	0.14	0.12	1.57	101
EA	0.2				0.14			174
FE					0.11	0.15	0.98	102
MS	0.18	0.15	0.61	0.55	0.14	0.12	1.57	100

*) Results of calculations without allowance for the repulsive barrier between layers
 **) Evaluated under the assumption that $\mu_{\perp} = 0.14$. MA—magnetic absorption, EA—electric absorption, σ —electrical conductivity, FE—Faraday effect, MS—magnetic Stark effect electrical conductivity, FE—Faraday effect, MS—magnetic Stark effect.

lating function, the integral over this function should go to zero as the spatial volume of integration grows, i.e., as the Bohr radius increases.

Let us now consider the question of the value of the anisotropy parameter $\gamma = \epsilon_{\perp} \mu_{\perp} / \epsilon_{\parallel} \mu_{\parallel}$ in layered GaSe crystals. To answer this question, one must know the values of the dielectric permittivities and of the reduced effective masses of the exciton. There is complete unanimity in the literature as to the values of ϵ_{\perp} and ϵ_{\parallel} . These values were measured by Leung *et al.*⁹⁹ as: $\epsilon_{\perp} = 10.2$, $\epsilon_{\parallel} = 7.6$. The situation in regard to the numerical values of the reduced effective masses of the exciton is quite another matter. Table VII gives the results of various theoretical calculations and the data of several experimental studies. In Ref. 100 the translational mass of the exciton, $M_{\parallel} = m_{\parallel}^e + m_{\parallel}^h = 0.7m_0$, was measured directly. The values of the other parameters given in this row of the table were calculated using the data of Refs. 64 and 101: $\mu_{\perp} = 0.14m_0$, $\mu_{\perp}/\mu_{\parallel} = 1.2$, and $\sigma = 4.3 \cdot 10^{-5}$ meV/kOe², where σ is the parameter characterizing the diamagnetic shift of the exciton levels. The good agreement among the values of the anisotropy parameters γ observed in these studies is therefore completely justified, but this agreement cannot serve as evidence of the correctness of the value $\gamma \sim 1.6$. The most complete and systematic analysis undertaken to determine the anisotropy parameter γ is that of Mooser and Schlüter.⁶⁴ Those authors made a very detailed study of the magnetic-field dependence of the absorption spectra of GaSe single crystals. The experiments were done in both the Faraday and Voigt geometries. In the Voigt geometry in large magnetic fields they detected a new line a little below the 2s state, which was identified as the 2p_y state (2p_x) of the exciton. By extrapolating the position of this line to zero magnetic field, they determined the ionization energy of this state

$$E_{2p_{\pm 1}} = -(5.5 \pm 0.1) \text{ meV.}$$

Using the results of the theoretical calculations of Harper and Hilder,⁷¹ which imply that

$$\frac{E_{2p_{\pm 1}} - E_{2s}}{E_{2s}} = \frac{(3/2) f^{\prime}(\gamma) - f^{00}(\gamma)}{f^{00}(\gamma) - 1},$$

where

$$f^{00}(\gamma) = \frac{1}{\sqrt{\gamma-1}} \ln \frac{\sqrt{\gamma} + \sqrt{\gamma-1}}{\sqrt{\gamma} - \sqrt{\gamma-1}},$$

$$f^{\prime}(\gamma) = \frac{1}{\sqrt{\gamma-1}} \left[1 + \frac{1}{2(\gamma-1)} \right] \ln \left(\frac{\sqrt{\gamma} + \sqrt{\gamma-1}}{\sqrt{\gamma} - \sqrt{\gamma-1}} \right) - \frac{\sqrt{\gamma}}{\gamma-1},$$

they evaluated the anisotropy parameter as $\gamma = 1.8$ ($E_{2s} = 5$ meV).⁶⁴ Since the ratio of dielectric permittivities $\epsilon_{\perp}/\epsilon_{\parallel} = 1.34$ (Ref. 99), for $\gamma = 1.8$ one has $\mu_{\perp}/\mu_{\parallel} = 1.3 \pm 0.2$. It follows from Ref. 73 that the binding energy of an exciton in the layered crystals is $E_{1s} = Ry^* [f^{00}(\gamma) - 1]$. Knowing γ , one can determine $\mu_{\perp} = 0.14m_0$ and $\mu_{\parallel} = 0.11m_0$.

The method proposed by Mooser and Schlüter⁶⁴ for determining the anisotropy parameter is very sensitive to the accuracy with which the energies $E_{2p_{\pm 1}}$ and E_{2s} are measured, and the value of $E_{2p_{\pm 1}}$ was estimated by extrapolating the energy position of the corresponding absorption line to zero magnetic field. If, for example, it is assumed that the measurement error in Ref. 64 is not more than ± 0.1 meV, then our estimates show that the scatter in the value of γ is ± 0.2 . It should also be noted that the value $\mu_{\perp}/\mu_{\parallel} = 1.3 \pm 0.2$ obtained for the ratio of the reduced effective masses of the exciton using $\gamma = 1.8$ is in disagreement with the results of measurements reported in Ref. 64. By comparing the values of the diamagnetic shift of the exciton level with $n = 2$ in the Voigt and Faraday geometries, the authors of Ref. 64 obtained $\mu_{\perp}/\mu_{\parallel} = 0.95$.

In view of the low accuracy of the magneto-optic measurements, the necessity of extrapolating to zero magnetic field, and the contradiction of certain of the results of Ref. 64, it becomes necessary to examine anew the question of the value of the anisotropy parameter in GaSe layered crystals. In considering this question, we shall proceed from the experimental data obtained by the most accurate direct measurements without any assumptions about any parameters except the values of ϵ_{\perp} and ϵ_{\parallel} in GaSe layered crystals. One can include in these data the reliably established fact that the energy spectrum of the triplet exciton in GaSe is purely hydrogen-like (Fig. 19), with an exciton binding energy $Ry = 19.9$ meV and a gap width $E_g = 2.1295$ eV. This result follows directly from an analysis of the absorption spectrum⁹⁰ (see Fig. 17) and the hot luminescence spectrum⁸⁶ (Fig. 20).

Further, the energy position of the exciton levels in a magnetic field was measured by the Faraday effect in Ref. 102. These measurements should be regarded as more accurate than the magnetic absorption results. This is because what is measured in a Faraday-effect

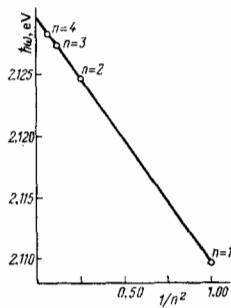


FIG. 19. Energies of 1s, 2s, 3s, and 4s exciton states in GaSe as functions of $1/n^2$.

experiment is the angle of rotation of the plane of polarization,

$$\theta \sim \frac{dn}{d\omega} \frac{d}{2c} \omega \omega_L,$$

where n is the index of refraction and $\omega_L = (1/2)g^* \mu_B H$, with g^* the effective g factor and μ_B the Bohr magneton. Measurements of this sort should be classed as differential, and differential measurements, as a rule, have a substantially better energy resolution.

Thus, the experimental data we shall use to determine the anisotropy parameter γ in GaSe are the following:

$$\left. \begin{aligned} Ry &= 19.9 \text{ meV,} \\ E_{n=1} &= 2.102 \text{ eV,} \\ E_{n=2} &= 2.119 \text{ eV} \end{aligned} \right\} \text{ in a magnetic field } H = 51 \text{ kOe.}$$

In addition, we shall use the results of Gerlach and Pollman⁷⁸ to determine the effective excitonic rydberg $Ry^* = \mu_{\perp} e^4 / 2\hbar^2 \epsilon_{\perp} \epsilon_{\parallel}$:

$$Z_{00}^2(\alpha) Ry^* = Ry,$$

where the function $Z_{00}(\alpha)$ is given in Table VI. The theory of Ref. 78 should be valid in the case of GaSe crystals since the excitonic energy spectrum, as we have already mentioned, is purely hydrogenic, in agreement with the main implication of this theory.

We shall also take into account the dependence⁷⁹ of the diamagnetic shift on the anisotropy parameter $\alpha = 1 - \gamma$:

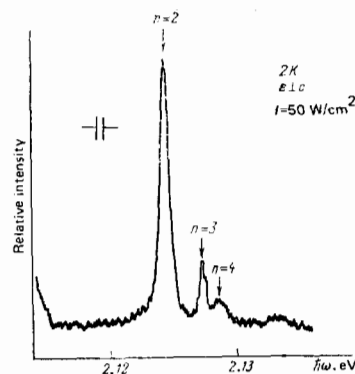


FIG. 20. Hot luminescence spectrum of GaSe at $T=2$ K for an excitation level $I=50$ W/cm^2 .

TABLE VIII.

γ	μ_{\perp}/m_0	μ_{\parallel}/m_0	Ry*, meV	Ry, meV	σ_0 , meV/kOe ²	σ_0^* , Å
1.12	0.12	0.14	20.7	19.9	$6.14 \cdot 10^{-5}$	38.8

$$\Delta E_{\parallel}(\alpha, H_z) = \frac{n^2 [5n^2 - 3l(l+1) + 4] [l(l+1) + m^2 - 1]}{2(2l+3)(2l-1)} \frac{\sigma H_z}{Z_{lm}^2(\alpha)}, \quad (23)$$

where $\sigma = (e^2/4\mu_{\perp}c^2)(a_0^*)^2$, with a_0^* being the effective Bohr radius of the exciton. This dependence is explained by the fact that the "real" Bohr radius, which should be substituted into the expression for σ is, like the excitonic Ry, determined by the anisotropy of the crystal. Therefore, the initial equations are written as follows:

$$\begin{aligned} Ry &= Ry^* Z_{00}^2(\alpha), \\ E_{1s} &= E_R(H) - Ry + \frac{\sigma H^2}{Z_{00}^2(\alpha)}, \\ E_{2s} &= E_g(H) - \frac{Ry}{4} + 14 \frac{\sigma H^2}{Z_{00}^2(\alpha)}. \end{aligned}$$

Subtracting the second equation from the third, we obtain a system of two equations in the two unknowns $Z_{00}^2(\alpha)$ and μ_{\perp} :

$$\begin{aligned} Ry &= Ry^* Z_{00}^2(\alpha), \\ E_{2s} - E_{1s} &= \frac{3}{4} Ry + \frac{13\sigma H^2}{Z_{00}^2(\alpha)}. \end{aligned}$$

Solving this system of equations, we obtain $Z_{00}^2(\alpha) = 0.96$ and $\mu_{\perp} = 0.12m_0$. From the value $Z_{00}^2(\alpha) = [(1/\sqrt{\alpha}) \text{Arc sinh } \sqrt{1/\alpha}]^2$ (see Table VI) we evaluate the anisotropy parameter $\gamma = 1.12$ and the other parameters given in Table VIII for the excitonic states in GaSe layered crystals. Unfortunately, the available data on the exciton spectra of other III-VI crystals (InSe,¹⁰³⁻¹⁰⁷ GaTe,¹⁰⁸⁻¹¹² and GaS¹¹³⁻¹¹⁶) are less complete, and it is not possible at the present time to analyze the properties of the exciton states in these crystals as we have just done for GaSe.

6. ELECTRONIC CHARGE-DENSITY DISTRIBUTION IN III-VI LAYERED SEMICONDUCTORS

We have thus seen that the exciton states near the absorption edge ($K=0$) in gallium selenide display three-dimensional properties. At the same time, the vibrational spectra of this same material have properties which are typical of two-dimensional crystals.

The reason for this state of affairs was pointed out by Schlüter,^{11,117} who calculated the band structure of gallium selenide (Fig. 21) by an empirical pseudopotential method. According to Schlüter,¹¹ the energy states in GaSe can be divided into two types: 1) states with wave functions concentrated mainly around and between Ga atoms within an individual layer; 2) states with wave functions which include the p_x orbitals of Se atoms located on the boundary of adjacent layers and are therefore concentrated to a large degree in the space between the adjacent layers.

The states of the first type have a small "width" in the direction of the C axis of the hexagonal Brillouin zone; for these states the effective masses m_{\parallel} describing the motion of the carriers parallel to the C axis of

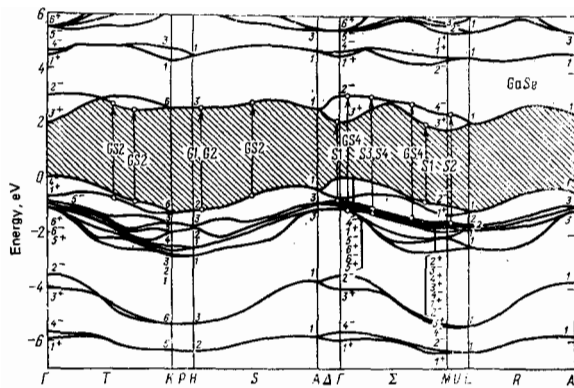


FIG. 21. Band structure of gallium selenide as calculated by the pseudopotential method. The indicated transitions correspond to the main structures of the reflection spectrum of GaSe (5 K, $E \perp C$). The letters on the arrows indicate the magnitude of the energy shift Δ of the optical transition when the selenium is completely replaced by sulfur: $G - \Delta = 0$, $GS - \Delta \approx 400$ meV, $S - \Delta = 780$ meV (Ref. 117).

the crystal are large—the corresponding bands are two-dimensional.

The bands of the second type are three-dimensional and are characterized by relatively small effective masses m_{ii} . The orbitals of the atoms on the two neighboring layers contribute to the corresponding electron density, and the overlap of these orbitals is determined to a large extent by the strength of the interaction between the layers and the frequencies of the interlayer oscillations.

The edge excitons at $K=0$ are three dimensional in GaSe because the highest valence band of symmetry Γ_4^- and the lowest conduction band Γ_3^+ are both states of the second type, made up largely of the p_x orbitals of the selenium atoms.

One can obtain experimental information on the nature of a band by examining the changes in the energy spectrum of the crystal upon the systematic substitution of other cations and anions. For this one must have at his disposal a continuous series of solid solutions based on the crystal under study and be able to track the energy positions of the bands of interest. Single crystals of the gallium-selenide based solid solutions GaS_xSe_{1-x} , $GaTe_xSe_{1-x}$, and $In_xGa_{1-x}Se$ turned out to be a fortunate choice as objects of study in this regard. According to structural studies¹¹⁶⁻¹²⁰ and studies of the Raman-scattering spectra,¹²¹ these crystals have the same crystal structure as the ϵ polytype of GaSe, at least for compositions in the range $0 \leq x \leq 0.2$. The absorption and luminescence spectra of all these semiconductors clearly display narrow lines that are judged from their shape and the temperature dependence of their intensity to be due to excitonic transitions occurring without a change in the wave vector, while their polarization properties correspond to the $\Gamma_4^- \rightarrow \Gamma_3^+$ transitions in gallium selenide.^{119, 122-127} Figure 22 shows how the energy of the direct-exciton band depends on the compositions of the GaSe-analog crystals. The experiments¹²⁸ were done at

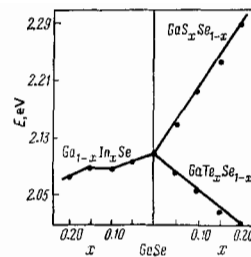


FIG. 22. Energy of exciton band at $K=0$ as a function of the composition of GaSe-analog crystals (4.2 K, $E \perp C$).

4.2 K. Cation substitution (In for Ga) has a smaller effect on the position of E_{exc} than does anion substitution (S and Te for Se), in agreement with the conclusions of Schlüter¹¹ that the anion orbitals give the predominant contribution to the electron density of the states which play the role of the top of the valence band and the bottom of the conduction band at the center of the Brillouin zone in GaSe and its analogs.

More complete information on the nature of the various electronic states in gallium selenide has been obtained in studies^{117, 129} of the optical spectra of GaS_xSe_{1-x} crystals with $0 \leq x \leq 1$. It was found¹²⁹ that the substitution of S for Se causes substantially different changes in the energies of the direct and indirect transitions. While the total value of the energy shift for the direct transitions was found to be $\Delta \sim 900$ meV, the corresponding shift of the indirect absorption edge (the transition $\Gamma_4^- \rightarrow M_3^+$) is $\Delta = 400$ meV (Fig. 23). Based on the fact that the energy position of the bottom of the conduction band at the point M depends relatively weakly on the anion composition of the crystal, the conclusion was reached that the contribution of the cation orbitals to the corresponding electron density can be appreciable, and for this reason the anisotropy of the excitons (the indirect transition $\Gamma_4^- \rightarrow M_3^+$) in GaS, for example, can be substantial.^{130, 124}

This approach was developed further in an analysis of the results of experimental studies of the reflection spectra of GaS_xSe_{1-x} crystals in the 3–6 eV region of the spectrum at a temperature of 4.2 K. After finding the linear shift of the energy position of the most char-

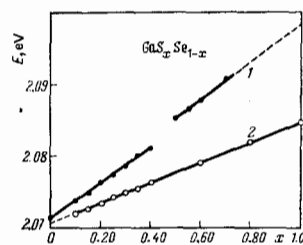


FIG. 23. Energy of excitonic absorption peak (1) and the position of the short-wavelength line in the photoluminescence spectrum of GaS_xSe_{1-x} as functions of the composition x (4.2 K, $E \perp C$). Curve 1 corresponds to the change in the energy of the direct transitions ($\Gamma_4^- \rightarrow \Gamma_3^+$), curve 2 to the change in the energy of the indirect ($\Gamma_4^- \rightarrow M_3^+$) transitions.

acteristic structures in the reflection spectra of the series of crystals $\text{GaS}_x\text{Se}_{1-x}$ ($0 \leq x \leq 1$) and comparing each peak with the corresponding optical transition, Schlüter and co-workers¹¹⁷ grouped the structures into three different classes: those with a strong shift (e.g., the $\Gamma_3^* \rightarrow \Gamma_4^-$ transition); those with an intermediate shift ($\Delta \sim 400$ meV, e.g., $\Gamma_3^* \rightarrow M_3^*$); and, finally, those with no shift ($H_2 \rightarrow H_3$). They were able to trace the correspondence between the size of the change (Δ) in the transition energy and the relative contribution of the anion (or cation) orbitals to the electron density of the initial and final states of the transition. This correspondence is illustrated by the charge-density contour maps^{11,13,117} obtained by plotting the value of $\rho(\mathbf{r}) = 2e|\psi_{\mathbf{k}}(\mathbf{r})|^2$ in a given plane in real space (here $\psi_{\mathbf{k}}$ is the wave function with wave vector \mathbf{k} for the given band, normalized in such a way¹¹⁷ that $|\psi(\mathbf{r})|^2 = 1/\Omega$, where Ω is the volume of the unit cell). The contour maps for the (110) plane are shown in Figs. 24, 25, and 26; the numbers on the maps give the value of $\rho(\mathbf{r})$ at the corresponding points on this plane.

If the transition energy remains unchanged when the composition of the $\text{GaS}_x\text{Se}_{1-x}$ crystals is changed, the electron densities characterizing the initial and final states of the transition are formed without much of a contribution from the anion charge (see Fig. 23), and it is primarily the Ga-Ga band within an individual layer that is excited in the optical transition. In the intermediate case ($\Delta \sim 400$ meV) the charge distribution has a mixed cation-anion character, and it is to this class of transitions that the indirect transitions $\Gamma_3^* \rightarrow M_3^*$ belong (Fig. 25a,c). Finally, the large value of Δ for the energies of the direct transitions $\Gamma_3^* \rightarrow \Gamma_4^-$ at the absorption edge in gallium selenide and its analogs is due to the contribution of anion orbitals located between the layers (Fig. 25a,b).

The idea that the anisotropy of the states is determined by the size of the contribution to the corresponding electron density from the anion p_x orbitals located between the layers is supported by the results of angle-resolved photoemission studies.

The dispersion of the energy bands is investigated in these studies in the following way.^{132,133} One measures

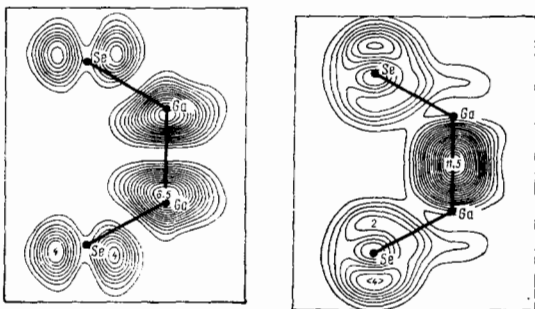


FIG. 24. Contour maps of the charge density corresponding to the states which play the role of the top of the valence band (the lower map) and the bottom of the conduction band (upper map) at the point H of the Brillouin zone.¹¹⁷ This transition is denoted G1, G2 in Fig. 21.

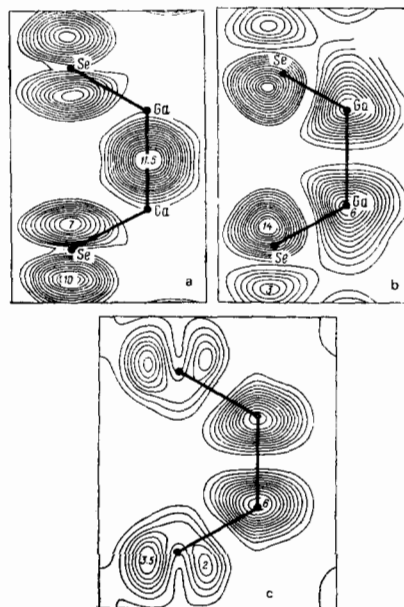


FIG. 25. Contour maps of the charge density corresponding to the states which in gallium selenide play the roles of the top of the valence band Γ_4^- (a), of the bottom of the conduction band at the center of the Brillouin zone Γ_3^+ (b) and at the zone edge M_3^+ (c) (Ref. 117).

the kinetic energy E of the electrons photoemitted into vacuum at different angles to the surface, defining the polar angle θ as the angle between the trajectory of the electron and the outward normal to the surface, and the azimuthal angle φ as the angle of rotation about this normal. Directing the z axis perpendicular to the surface of the crystal, one can relate the components $k'_x = \sqrt{2mE/\hbar^2} \sin\theta \cos\varphi$, $k'_y = \sqrt{2mE/\hbar^2} \sin\theta \sin\varphi$, $k'_z = \sqrt{2mE/\hbar^2}$ of the wave vector in the vacuum to the components k_x, k_y, k_z in the crystal, assuming that the refraction of the electron wave at the intersection with the boundary of the crystal occurs in such a way that k_x and k_y are conserved to within a reciprocal-lattice vector. The dispersion is characterized by the experimentally

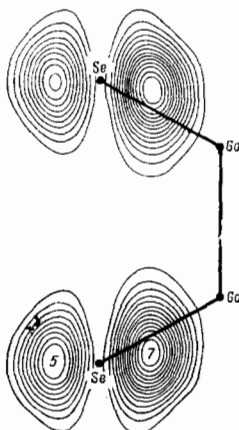


FIG. 26. Contour map of the charge density corresponding to each of the two-dimensional states Γ_5^+ , Γ_5^- , Γ_6^+ , and Γ_6^- in the valence band of gallium selenide.¹¹⁷

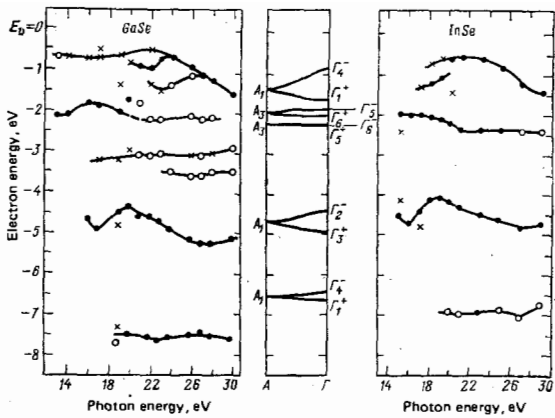


FIG. 27. Comparison of the results of photoemission studies of the crystals GaSe and InSe with the band structure constructed by Schlüter¹¹ for gallium selenide (in the center). The experiments measured the energy positions of the characteristics of the peaks in the photoemission spectrum as a function of the incident photon energy.¹³⁴

determined dependence of the initial-state energy $E_i = \hbar\omega - E - W$ on the wave vector $k_{\parallel} = \sqrt{k_x^2 + k_y^2} = \sqrt{2mE_x/\hbar^2} \sin\theta$ ($\hbar\omega$ is the energy of the incident photon, E is the kinetic energy of the escaping electron, and W is the work function). The dispersion of the bands along the k_x direction (in the case of a crystal with hexagonal symmetry this is the $\Gamma - \Delta - A$ direction in the Brillouin zone) is studied independently by examining the energy spectrum of the electrons emitted normal to the surface as a function of the incident photon energy. As a source of monochromatic radiation one usually uses the storage ring of a synchrotron. Any change detected in the energy of the corresponding peak as the photon energy is changed is assumed to be due to dispersion of the band along the k_x direction. This method has been used¹³³ to study the energy structure of the bands in graphite and PbI_2 .

In Fig. 27 the results of photoemission studies^{134,135} of gallium selenide and indium selenide are compared with the energy structure of gallium selenide calculated by Schlüter and co-workers.^{11,117} The initial energy was taken to be the energy E_v at the top of the valence band as determined from the threshold value of the energy of the emitted electrons. It is clearly seen that the highest group of valence bands $\Gamma_4^-\Gamma_1^+$, the optical transitions from which form the absorption edge in GaSe and InSe, displays a considerable dispersion (~ 1 eV) along the direction perpendicular to the layers of the crystal. According to the data of Ref. 11, these three-dimensional states are characterized by a significant contribution to the corresponding electron density from the p_x orbitals of selenium. The group of two-dimensional bands $\Gamma_5^+, \Gamma_5^-\Gamma_6^+, \Gamma_6^-$ is characterized by a weak dispersion along k_x (< 0.3). These states display a predominantly $p_{x,y}$ character (Fig. 26). The degree to which p_x -like charges, which are localized about the Se atoms, are mixed in determines the different values of the dispersion for the deeper states $\Gamma_2^-\Gamma_3^+$ and $\Gamma_1^-\Gamma_4^-$ (Ref. 134).

7. CONCLUSION

In summary, the electronic states in layered crystals can be both two- and three-dimensional. The existence of isotropic electronic states in gallium selenide and its analogs is due to the overlap from one layer to the next of the anion p_x orbitals, which contribute the most to the the corresponding electron density. The degree of overlap of these orbitals determines the value of the elastic constants characterizing the intralayer oscillations (see Sect. 3). At the same time, the orbitals of the metal and the $p_{x,y}$ orbitals of the chalcogenides, which overlap weakly between layers, form an electron density which corresponds to highly anisotropic and two-dimensional states; the magnitude and distribution of the electronic charge density concentrated between individual atoms of the layer characterize the frequencies of the intralayer phonon modes.

The three-dimensionality of the states which play the role of the top of the valence band and the bottom of the conduction band at $K=0$ in gallium selenide and its analogs determines the isotropic character of the corresponding exciton bands and cannot be invoked to explain the anisotropy of the electrical properties that has been detected in various experiments.^{96,136-139} The ratio of the conductivities in the directions parallel to and perpendicular to the layers can reach three orders of magnitude in gallium selenide, for example. The observed anisotropy of the electrical properties can be understood by keeping in mind that in a real layered crystal the conductivity perpendicular to the layers is governed by the large number of structural defects: dislocations located in the basal plane of the layer and defects in the stacking of the layers, which have a low energy of formation.¹⁴⁰⁻¹⁴³ The conductivity of such a system in the direction perpendicular to the plane in which the defects lie can have a singular character:⁹⁶ a detailed discussion of this phenomenon, however, is beyond the scope of this paper. The results of Refs. 96 and 136-139 are consistent with a three-dimensional character of the above-named electronic states; they are also consistent with the results of pseudopotential calculations,^{11,137} confirmed by optical experiments, as to the ordering sequence of the bands of different anisotropy.

The two-dimensional ($\Gamma_{5,6}^-$) and highly anisotropic (e.g., M_3^+) bands are separated from the three-dimensional bands in gallium selenide by a small energy gap (see Fig. 20). This situation lends interest to the study of the effect of external influences on the physical properties of GaSe and its analogs. Since the deformation potentials for the bands of different anisotropy in these crystals differ in both sign and magnitude,^{11,144-147} the hope remains that for certain temperatures and conditions of uniaxial strain the highly anisotropic states can play a governing role in the investigation of exciton effects and charge transport processes.

The definite promise that such a situation can be realized stems from the study of various classes of semiconductors with a layered type of crystal structure,³⁻⁵ in particular multicomponent crystals whose layers have a complex structure.¹⁴⁸⁻¹⁵⁰ An example of such a crystal is TlGaSe_2 (whose unit cell contains 36

atoms and includes two layers with seven planes of atoms each). The optical spectra of these crystals at the absorption edge are interpreted in the framework of a model which includes excitonic transitions, the polarization properties of which are described in terms of the symmetry of only one layer.¹⁵¹

The energy spectrum of a layered crystal can be rearranged by introducing planar organic molecules such as pyridine between the layers. Intercalated structures created on the basis of graphite and transition-metal dichalcogenides have been studied intensively in recent years in connection with the problems of high-temperature superconductivity and the creation of dry sources of current.^{53, 152-154} These are data, confirmed by structural studies, on the intercalation of gallium selenide through anodic reactions occurring in an electrolytic solution of HgI₂ in ethylene glycol.¹⁵⁵ The physical properties of layered crystals intercalated with organic molecules were studied in Refs. 156-159. Finally, an extremely anisotropic spectrum can be achieved by localizing the excitons or carriers in one or several layers by reducing the thickness of the crystal. With layered crystals one can obtain thicknesses of only a few (3-5) layers. Here both the wave functions and the energy spectrum change on account of dimensional effects (see, for example, the paper by Harper and Hilder¹⁶⁰). The theory of Ref. 160, however, is in quantitative disagreement with the results of experiments conducted on the crystals of 2H-MoS₂ (Ref. 161), WSe₂ (Refs. 162 and 163), and GaSe (Ref. 164). An important step forward in the understanding of this question was taken by Keldysh,¹⁶⁵ who showed that when the thickness of the crystal is reduced to $d \lesssim a_0$ the Coulomb interaction between the electron and hole should increase if the dielectric permittivity of the surrounding medium is noticeably smaller than that of the crystal, leading to the growth of the binding energy of the exciton and to a change in its energy spectrum.

Thus, the possibilities presented by layered crystals for the study of a variety of new effects in solid-state physics are far from exhausted, and interest in these compounds is continually growing.

We are grateful to L. V. Keldysh for reading and discussing the manuscript and to R. Guseinov and R. Suleimanov for helpful remarks concerning specific parts of this review.

¹V. L. Ginzburg, Phys. Lett. **13**, 101 (1964).

²W. A. Little, Phys. Rev. **134**, A1416 (1964).

³E. Mooser, editor, Physics and Chemistry of Materials and Layered Structures, Reidel, Boston; Dordrecht, Holland (1976).

⁴I. Ch. Schlüter and M. Schlüter, Phys. Status Solidi B **57**, 145 (1973).

⁵L. N. Bulaevskii, Usp. Fiz. Nauk **116**, 449 (1975) [Sov. Phys. Usp. **18**, 514 (1975)].

⁶M. P. Lisitsa, Zh. Prikl. Spektrosk. **27**, 589 (1977).

⁷N. G. Basov, O. V. Bogdankevich, A. N. Pechenov, G. B. Abdullaev, G. A. Akhundov, and É. Yu. Salaev, Dokl. Akad. Nauk SSSR **161**, 1059 (1965) [Sov. Phys. Dokl. **10**, 329 (1965)].

⁸G. B. Abdullaev, L. A. Kulevskii, A. M. Prokhorov, A. D. Savel'ev, É. Yu. Salaev, and V. V. Smirnov, Pis'ma Zh. Eksp. Teor. Fiz. **16**, 130 (1972) [JETP Lett. **16**, 90 (1972)].

⁹G. B. Abdullaev, É. Yu. Salaev, and V. M. Salmanov, Vzaimodeistvie lazernogo islucheniya s poluprovodnikami tipa A³B⁶ [Interaction of Laser Radiation with III-VI semiconductors], Elm, Baku (1979).

¹⁰L. N. Kurbatov, A. A. Bylychenko, V. D. Bakumenko, V. A. Morozov, V. F. Chishko, and S. S. Makhidzhanov, Pis'ma Zh. Tekh. Fiz. **4**, 111 (1978) [Sov. Tech. Phys. Lett. **4**, 46 (1978)].

¹¹M. Schlüter, Nuovo Vimento B **13**, 313 (1973).

¹²J. B. Nelson and D. P. Riley, Proc. Phys. Soc., London **57**, 477 (1945).

¹³E. Mooser, J. C. Schlüter, and M. Schlüter, J. Phys. Chem. Solids **35**, 1269 (1974).

¹⁴V. B. Sapre and C. Mande, J. Phys. Chem. Solids **34**, 1351 (1973).

¹⁵A. Kuhn, A. Chevy, and R. Chevalier, Phys. Status Solidi A **31**, 469 (1975).

¹⁶R. W. G. Sycopf, Crystal Structure, Interscience, New York (1965).

¹⁷S. A. Semiletov and V. A. Vlasov, Kristallografiya **8**, 877 (1963) [Sov. Phys. Crystallogr. **8**, 704 (1964)].

¹⁸P. Likforman, A. D. Carre, J. E. Etienne, and B. Bachet, Acta Crystallogr. Sect. B **31**, 1252 (1975).

¹⁹K. C. Nagral and S. Z. Ali, Indian J. Appl. Phys. **14**, 434 (1976).

²⁰W. Pearson, Acta Crystallogr. **17**, 13 (1964).

²¹V. Grasso, G. Mondio, M. A. Pirrone, and G. Saitta, J. Phys. C **8**, 80 (1975).

²²L. N. Alieva, G. L. Belen'kiĭ, I. I. Reshina, É. Yu. Salaev, and V. Ya. Shteĭnshraĭber, Fiz. Tverd. Tela (Leningrad) **21**, 155 (1979) [Sov. Phys. Solid State **21**, 90 (1979)].

²³T. J. Wieting, Solid State Commun. **12**, 931 (1972).

²⁴J. A. Wilson and A. D. Yoffe, Adv. Phys. **18**, 193 (1969).

²⁵R. Nicklov, N. Wakabayashi, and H. G. Smith, Phys. Rev. B **5**, 4951 (1972).

²⁶F. Zallen, M. L. Slade, and A. T. Ward, Phys. Rev. B **3**, 4257 (1971).

²⁷M. P. Lisita, A. M. Yaremko, G. G. Tarasov, M. Ya. Valakh, and L. I. Berizhinskiĭ, Fiz. Tverd. Tela (Leningrad) **14**, 3219 (1972) [Sov. Phys. Solid State **14**, 2744 (1973)].

²⁸J. L. Verble, T. J. Wieting, and P. R. Read, Solid State Commun. **11**, 941 (1972).

²⁹T. J. Wieting and J. L. Verble, Phys. Rev. B **5**, 1473 (1972).

³⁰M. Hayek, O. Brafman, and R. A. M. Lieth, Phys. Rev. B **8**, 2772 (1973).

³¹J. P. Van der Ziel, A. E. Meixnar, and H. M. Kasper, Solid State Commun. **12**, 1213 (1973).

³²G. L. Belen'kiĭ, É. Yu. Salaev, R. A. Suleimanov, and L. N. Alieva, Izv. Akad. Nauk Az. SSR Ser. Fiz.-Tekh. Mat. Nauk, No. 4, 60 (1978).

³³L. K. Vodop'yanov, L. V. Golubev, Yu. A. Aleshchenko, K. R. Allakhverdiev, and E. Yu. Salaev, Fiz. Tverd. Tela (Leningrad) **20**, 2803 (1978) [Sov. Phys. Solid State **20**, 1618 (1978)].

³⁴S. Jandle and C. Carlone, Solid State Commun. **25**, 5 (1978).

³⁵J. M. Besson, Nuovo Cimento B **38**, 488 (1977).

³⁶R. Zallen and M. Slade, Phys. Rev. B **9**, 1627 (1974).

³⁷A. S. Davydov, Teoriya molekulyarnykh éksitonov, Nauka, Moscow (1968) [Theory of Molecular Excitons, McGraw-Hill, New York (1962)].

³⁸V. V. Artamonov, M. Ya. Valakh, and M. P. Lisitsa, Phys. Status Solidi B **105**, K103 (1981).

³⁹S. Jandle, J. L. Brebner, and B. M. Powell, Phys. Rev. B **13**, 658 (1976).

⁴⁰B. M. Powell, S. Jandle, and J. L. Brebner, J. Phys. C **10**, 3039 (1977).

- ⁴¹Z. A. Iskender-Zade, V. D. Faradzhev, and A. I. Agaev, *Fiz. Tverd. Tela (Leningrad)* **19**, 851 (1977) [*Sov. Phys. Solid State* **19**, 492 (1977)].
- ⁴²N. Wakabayashi, H. G. Smith, and R. M. Nicklov, *Phys. Rev. B* **12**, 659 (1975).
- ⁴³V. K. Bashenov, Q. Bayman, B. I. Marvakov, *Phys. Status Solidi B* **82**, 705 (1977).
- ⁴⁴G. L. Belenkii, L. N. Alieva, R. Kh. Nani, and E. Yu. Salaev, *Phys. Status Solidi B* **82**, 805 (1977).
- ⁴⁵A. Polian and K. Kunc, *Solid State Commun.* **12**, 1079 (1976); *J. Phys. (Paris)* **42**, 295 (1981).
- ⁴⁶K. K. Mamedov, M. A. Aldzhanov, I. G. Kerimov, and M. I. Mekhtiev, *Fiz. Tverd. Tela (Leningrad)* **20**, 42 (1978) [*Sov. Phys. Solid State* **20**, 22 (1978)].
- ⁴⁷K. K. Mamedov, I. G. Kerimov, V. N. Kostyukov, and G. G. A. Guseinov, *Zh. Fiz. Khim.* **41**, 1300 (1967).
- ⁴⁸I. M. Lifshits, *Zh. Eksp. Teor. Fiz.* **22**, 475 (1952).
- ⁴⁹N. Wakabayashi, *Nuovo Cimento B* **38**, 256 (1977).
- ⁵⁰G. L. Belen'kii, L. N. Alieva, N. Kh. Nani, É. Yu. Salaev, and V. Ya. Shteinshraiber, *Fiz. Tverd. Tela (Leningrad)* **19**, 282 (1977) [*Sov. Phys. Solid State* **19**, 162 (1977)].
- ⁵¹I. C. Irwin, B. P. Clayman, and D. G. Mead, *Phys. Rev. B* **19**, 2099 (1979).
- ⁵²G. B. Abdullaev, L. K. Vodopyanov, K. R. Allakhverdiev, L. Golubev, S. S. Babaev, and É. Yu. Salaev, *Solid State Commun.* **31**, 851 (1979).
- ⁵³V. L. Ginzburg and D. A. Kirzhints, editors, *Problemy vysokotemperaturnoi sverkhprovodimosti [Problems in High-Temperature Superconductivity]*, Nauka, Moscow (1977).
- ⁵⁴E. A. Andryushin, L. V. Keldysh, and A. P. Silin, *Zh. Eksp. Teor. Fiz.* **73**, 1163 (1977) [*Sov. Phys. JETP* **46**, 616 (1977)].
- ⁵⁵J. A. Wilson and A. D. Yoffe, *Adv. Phys.* **18**, 193 (1969).
- ⁵⁶D. V. Bullet, *J. Phys. C* **11**, 4501 (1979).
- ⁵⁷G. Dresselhaus, *J. Phys. Chem. Solids* **1**, 14 (1956).
- ⁵⁸S. Flüge and E. Marshall, *Bechenmethoden der Quantentheorie*, Springer-Verlag, Berlin (1952).
- ⁵⁹B. Velicky and J. Sak, *Phys. Status Solidi* **16**, 147 (1966).
- ⁶⁰H. I. Ralph, *Solid State Commun.* **3**, 303 (1965).
- ⁶¹M. Shinada and S. Sugano, *J. Phys. Soc. Jpn.* **21**, 1936 (1966).
- ⁶²A. R. Beal, J. C. Knights, and W. Y. Liang, *J. Phys. C* **5**, 3540 (1972).
- ⁶³J. Bordas, *Physics and Chemistry of Matter with Layered Structure* **4**, 144 (1976).
- ⁶⁴E. Mooser and M. Schlüter, *Nuovo Cimento B* **18**, 164 (1973).
- ⁶⁵J. L. Brebner, *J. Phys. Chem. Solids* **25**, 1427 (1964).
- ⁶⁶J. L. Brebner and G. Fisher, *Can. J. Phys.* **41**, 561 (1963).
- ⁶⁷G. L. Bir and G. E. Pikus, *Simmetriya i deformatsionnye efekty v poluprovodnikakh*, Nauka, Moscow (1972) [Symmetry and Strain-Induced Effects in Semiconductors, Israel Program for Scientific Translations, Jerusalem; Wiley, New York (1975)].
- ⁶⁸W. Kohn and J. M. Luttinger, *Phys. Rev.* **98**, 915 (1955).
- ⁶⁹J. J. Hopfield and D. G. Thomas, *Phys. Rev.* **122**, 35 (1961).
- ⁷⁰R. Wheeler and J. O. Dimmock, *Phys. Rev.* **125**, 1805 (1962).
- ⁷¹P. G. Harper and J. A. Hilder, *Phys. Status Solidi* **26**, 69 (1968).
- ⁷²R. A. Daulkner, *Phys. Rev.* **184**, 713 (1969).
- ⁷³J. A. Déverin, *Helv. Phys. Acta* **42**, 397 (1969).
- ⁷⁴J. A. Déverin, *Nuovo Cimento B* **63**, 1 (1969).
- ⁷⁵A. Baldereschi and M. G. Diaz, *Nuovo Cimento B* **69**, 217 (1970).
- ⁷⁶R. Zimmerman, *Phys. Status Solidi B* **46**, K111 (1971).
- ⁷⁷J. Pollman, *Phys. Status Solidi B* **63**, 501 (1974).
- ⁷⁸B. Gerlach and J. Pollman, *Phys. Status Solidi B* **67**, 93 (1975).
- ⁷⁹B. Gerlach and J. Pollman, *Phys. Status Solidi B* **67**, 477 (1975).
- ⁸⁰J. Pollman, *Solid State Commun.* **19**, 361 (1976).
- ⁸¹B. Gerlach and J. Pollman, *Nuovo Cimento B* **38**, 423 (1977).
- ⁸²J. K. L. McDonald, *Phys. Rev.* **43**, 830 (1933).
- ⁸⁴A. Mercier, E. Mooser, and J. P. Voitchovsky, *J. Lumin.* **77**, 241 (1973).
- ⁸⁵J. P. Voitchovsky and A. Mercier, *Nuovo Cimento B* **22**, 27 (1974).
- ⁸⁶V. S. Bagaev, G. L. Belen'kii, V. V. Zaitsev, É. Yu. Salaev, and V. V. Stopachinskiĭ, *Fiz. Tverd. Tela (Leningrad)* **21**, 2217 (1979) [*Sov. Phys. Solid State* **21**, 1275 (1979)].
- ⁸⁷P. Dawson, K. Morigaki, and B. C. Cavenett, in: *Proc. Fourteenth Intern. Conf. on Physics of Semiconductors, Edinburgh, 1978*, publ. by Institute of Physics, London (1979), p. 1023.
- ⁸⁸K. Morigaki, P. Dawson, and B. C. Cavenett, *Solid State Commun.* **28**, 829 (1978).
- ⁸⁹B. C. Cavenett, P. Dawson, and K. Morigaki, *J. Phys. C* **12**, L197 (1979).
- ⁹⁰J. L. Brebner, G. Halpern, and E. Mooser, *Helv. Phys. Acta* **40**, 382 (1967).
- ⁹¹J. L. Brebner and E. Mooser, *Phys. Lett. A* **24**, 274 (1967).
- ⁹²T. Le Chi, Y. Depeursinge, F. Levy, and E. Mooser, *J. Phys. Chem. Solids* **36**, 699 (1975).
- ⁹³N. Kuroda and Y. Nishina, *Nuovo Cimento B* **32**, 109 (1976).
- ⁹⁴Y. Depeursinge, *Nuovo Cimento B* **38**, 153 (1977).
- ⁹⁵H. Kamimura and N. Nakao, *J. Phys. Soc. Jpn.* **21**, Suppl. p. 27 (1966).
- ⁹⁶Maschke and Ph. Schmid, *Phys. Rev. B* **12**, 4312 (1975).
- ⁹⁷J. J. Forney, K. Maschke, and E. Mooser, *J. Phys. C* **10**, 1887 (1977).
- ⁹⁸J. J. Forney, K. Maschke, and E. Mooser, *Nuovo Cimento B* **38**, 418 (1977).
- ⁹⁹P. C. Leung, G. Anderman, W. C. Spitzer, and C. A. Mead, *J. Phys. Chem. Solids* **27**, 849 (1966).
- ¹⁰⁰B. S. Razbirin, A. N. Starukhin, E. M. Gamarts, M. I. Karaman, and V. P. Mushinskiĭ, *Pis'ma Zh. Eksp. Teor. Fiz.* **27**, 341 (1978) [*JETP Lett.* **27**, 321 (1978)].
- ¹⁰¹G. Ottaviani, C. Canali, F. Nava, P. Schmid, E. Mooser, R. Minder, and I. Zschokke, *Solid State Commun.* **14**, 933 (1974).
- ¹⁰²D. Bianchi, U. Emilliani, and P. Podini, *Phys. Status Solidi B* **68**, 435 (1975).
- ¹⁰³M. V. Andriyshik, M. Yu. Sakhnovskii, V. B. Timofeev, and A. S. Yakimova, *Phys. Status Solidi B* **28**, 277 (1968).
- ¹⁰⁴V. L. Bakumenko, A. I. Dirochka, Z. D. Kovalyuk, L. N. Kurbatov, D. V. Sobolev, and V. F. Chishko, *Fiz. Tekh. Poluprovodn.* **8**, 1016 (1974) [*Sov. Phys. Semicond.* **8**, 660 (1974)].
- ¹⁰⁵J. Camassel, P. Merle, and H. Mathieu, *Phys. Rev. B* **17**, 4718 (1978).
- ¹⁰⁶Y. Depeursinge, E. Doni, R. Girlanda, A. Baldereschi, and K. Maschke, *Solid State Commun.* **27**, 1449 (1978).
- ¹⁰⁷N. Kuroda and Y. Nishina, *Physica (Utrecht) Ser. B* **105**, 30 (1981).
- ¹⁰⁸A. I. Dirochka, L. N. Kurbatov, and E. V. Sinitsyn, *Fiz. Tverd. Tela (Leningrad)* **17**, 2534 (1975) [*Sov. Phys. Solid State* **17**, 1690 (1975)].
- ¹⁰⁹U. Giorgiani, G. Mondio, P. Perillo, G. Saitta, and G. Vermiglio, *J. Phys. (Paris)* **38**, 1293 (1977).
- ¹¹⁰G. I. Abutalybov and M. L. Belle, *Fiz. Tekh. Poluprovodn.* **8**, 368 (1974) [*Sov. Phys. Semicond.* **8**, 234 (1974)].
- ¹¹¹J. Camassel, P. Merle, and H. Mathieu, *Physica (Utrecht) Ser. B+C* **99**, 309 (1980).
- ¹¹²L. N. Kurbatov, A. I. Dirochka, and V. A. Sosin, *Fiz. Tekh. Poluprovodn.* **13**, 75 (1979) [*Sov. Phys. Semicond.* **13**, 43 (1979)].
- ¹¹³Y. Sasaki, K. Hamaguchi, and Y. Nishina, *J. Phys. Soc. Jpn.* **50**, 1045 (1981).
- ¹¹⁴B. S. Razbirin, M. I. Karaman, V. P. Mushinskiĭ, and A. N. Starukhin, *Fiz. Tekh. Poluprovodn.* **7**, 1112 (1973) [*Sov. Phys. Semicond.* **7**, 753 (1973)].
- ¹¹⁵B. S. Razbirin, V. P. Mushinskiĭ, M. I. Karaman, A. N.

- Starukhin, and E. M. Gamarts, *Fiz. Tekh. Poluprovodn.* **12**, 33 (1978) [*Sov. Phys. Semicond.* **12**, 19 (1978)].
- ¹¹⁶G. L. Belenkii and M. O. Godzhaev, *Phys. Status Solidi B* **85**, 453 (1978).
- ¹¹⁷M. Schlüter, J. Camassel, S. Kohn, I. P. Voitchevsky, Y. R. Shen, and M. R. Cohen, *Phys. Rev. B* **13**, 3534 (1976).
- ¹¹⁸J. C. J. M. Terhell and R. M. A. Lieth, *Phys. Status Solidi A* **10**, 52 (1972).
- ¹¹⁹G. L. Belen'kiĭ, L. N. Alieva, M. A. Gezalov, R. Kh. Nani, É. Yu. Salaev, and R. A. Suleĭmanov, *Fiz. Tekh. Poluprovodn.* **12**, 106 (1978) [*Sov. Phys. Semicond.* **12**, 60 (1978)].
- ¹²⁰S. G. Abdullaeva and H. S. Mamedov, *Phys. Status Solidi B* **40**, K7 (1977).
- ¹²¹F. Cerdeira, E. A. Meneses, and A. Gousskov, *Phys. Rev. B* **16**, 1648 (1977).
- ¹²²S. G. Abdullaeva, G. L. Belen'kiĭ, R. Kh. Nani, É. Yu. Salaev, and R. A. Suleĭmanov, *Fiz. Takh. Poluprovodn.* **9**, 161 (1975) [*Sov. Phys. Semicond.* **9**, 108 (1975)].
- ¹²³L. N. Kurbatov, A. I. Dirochka, E. V. Sinitsyn, V. A. Sosin, M. I. Karaman, K. D. Kovalyuk, and V. P. Mushinskiĭ, *Izv. Akad. Nauk SSSR Ser. Fiz.* **40**, 2353 (1976).
- ¹²⁴N. Kuroda and Y. Nishina, *Phys. Status Solidi B* **81**, 72 (1975).
- ¹²⁵S. G. Abdullaeva, V. A. Gadgiev, T. G. Kerimova, and E. Yu. Salaev, *Nuovo Cimento B* **38**, 459 (1977).
- ¹²⁶J. Camassel, P. Merle, H. Mathieu, and A. Gousskov, *Phys. Rev. B* **19**, 1060 (1979).
- ¹²⁷G. L. Belenkii, M. O. Godghev, N. T. Mamedov, E. Yu. Salaev, and R. A. Sulimanov, *Phys. Status Solidi B* **53**, 137 (1979).
- ¹²⁸G. L. Belen'kiĭ, *Fiz. Tekh. Poluprovodn.* **13**, 406 (1979) [*Sov. Phys. Semicond.* **13**, 240 (1979)].
- ¹²⁹G. L. Belenkii, R. Kh. Nani, E. Yu. Salaev, and R. A. Suleĭmanov, *Phys. Status Solidi A* **31**, 707 (1975).
- ¹³⁰G. L. Belen'kiĭ, M. O. Godzhaev, and É. Yu. Salaev, *Pis'ma Zh. Eksp. Teor. Fiz.* **26**, 385 (1977) [*JETP Lett.* **26**, 263 (1977)].
- ¹³¹Y. Sasaki, K. Hamaguchi, and J. Nakai, *J. Phys. Soc. Jpn.* **38**, 1698 (1975).
- ¹³²N. V. Smith and M. M. Traum, *Phys. Rev. B* **11**, 2087 (1975).
- ¹³³P. M. Williams, *Nuovo Cimento B* **38**, 216 (1977).
- ¹³⁴P. K. Larsen, M. Schlüter, and N. V. Smith, *Solid State Commun.* **21**, 775 (1977).
- ¹³⁵P. K. Larsen, S. Chiang, and N. V. Smith, *Phys. Rev. B* **15**, 3200 (1977).
- ¹³⁶A. D. Yoffe, *Festkörperprobleme* **111**, 1 (1973).
- ¹³⁷A. H. M. Kipperman, A. I. Peynenborgh, and J. G. A. M. van der Dries, in: *Proc. Tenth Intern. Conf. on Physics of Semiconductors*, Cambridge, Mass., 1970, publ. by US Atomic Energy Commission, Washington, D.C. (1970), p. 822.
- ¹³⁸B. G. Tagiev and G. M. Mamedov, *Fiz. Tekh. Poluprovodn.* **8**, 1873 (1973) [*Sov. Phys. Semicond.* **8**, 1214 (1973)].
- ¹³⁹K. Maschke and H. Overhof, *Phys. Rev. B* **15**, 2058 (1977).
- ¹⁴⁰Z. S. Basinski, D. B. Dove, and E. Mooser, *J. Appl. Phys.* **34**, 469 (1963).
- ¹⁴¹E. Mooser and M. Schlüter, *Nuovo Cimento B* **18**, 164 (1973).
- ¹⁴²C. Monolikas and S. Amelinckx, *Physica (Utrecht) Ser. B+C* **99**, 31 (1980).
- ¹⁴³G. L. Belen'kiĭ, E. Yu. Salaev, and R. A. Suleĭmanov, *Fiz. Tverd. Tela (Leningrad)* **22**, 2525 (1980) [*Sov. Phys. Solid State* **22**, 1476 (1980)].
- ¹⁴⁴J. M. Besson, K. P. Jain, and A. Kuhn, *Phys. Rev. Lett.* **32**, 936 (1974).
- ¹⁴⁵G. L. Belen'kiĭ, É. I. Mirzoev, *Fiz. Tverd. Tela (Leningrad)* **22**, 3153 (1980) [*Sov. Phys. Solid State* **22**, 1842 (1980)].
- ¹⁴⁶G. L. Belenkii, E. Yu. Salaev, R. A. Suleĭmanov, and E. I. Mirzoev, *Phys. Status Solidi A* **63**, 97 (1981).
- ¹⁴⁷G. L. Belenkii and R. A. Suleĭmanov, *Solid State Commun.* **41**, 549 (1982).
- ¹⁴⁸D. Müller and H. Hanh, *Z. Anorg. Allg. Chem.* **438**, 258 (1978).
- ¹⁴⁹D. Müller, F. E. Poltman, and H. Hahn, *Z. Naturforsch. Teil B* **29**, 117 (1974).
- ¹⁵⁰T. I. Isaacs and R. H. Hopkins, *J. Crystal Growth* **29**, 121 (1975).
- ¹⁵¹S. G. Abdullaeva, G. L. Belen'kiĭ, and N. T. Mamedov, *Fiz. Tekh. Poluprovodn.* **15**, 943 (1981) [*Sov. Phys. Semicond.* **15**, 540 (1981)].
- ¹⁵²M. S. Dresselhaus and G. Dresselhaus, *Adv. Phys.* **30**, 139 (1981).
- ¹⁵³*Proc. Intern. Conf. on Layered Materials and Intercalates-3, Physica (Utrecht) Ser. B+C* **99**, 3-325 (1980).
- ¹⁵⁴V. L. Ginzburg, *Annu. Rev. Mater. Sci.* **2**, 663 (1972).
- ¹⁵⁵S. Ichimura, C. Tatsuyma, and O. Ueno, *Physica (Utrecht) Ser. B* **105**, 238 (1981).
- ¹⁵⁶D. V. Korbutyuk, V. A. Zuev, M. G. Ivaniĭchuk, V. G. Litovchenko, M. V. Kurik, and Z. D. Kovalyuk, *Fiz. Tekh. Poluprovodn.* **15** (1981) [*Sov. Phys. Semicond.* **15**, 327 (1981)].
- ¹⁵⁷Z. D. Kovalyuk and I. V. Mityanskiĭ, *Ukr. Fiz. Zh.* **27**, 616 (1982).
- ¹⁵⁸B. I. Verkin, B. Ya. Sukharevskiĭ, A. M. Gurevich, A. V. Alapina, and Yu. A. Dushchkin, *Fiz. Nizk. Temp.* **2**, 946 (1976) [*Sov. J. Low Temp. Phys.* **2**, 466 (1976)].
- ¹⁵⁹A. M. Gurevich, B. Ya. Sukharevskiĭ, and A. V. Alapina, *Fiz. Nizk. Temp.* **6**, 933 (1980) [*Sov. J. Low Temp. Phys.* **6**, 454 (1980)].
- ¹⁶⁰P. G. Harper and J. A. Hilder, *Phys. Status Solidi* **26**, 69 (1968).
- ¹⁶¹R. A. Neirlee and B. L. Evans, *Phys. Status Solidi B* **73**, 597 (1976).
- ¹⁶²D. J. Bradley, Y. Katayawa, and B. L. Evans, *Solid State Commun.* **11**, 1695 (1972).
- ¹⁶³F. Consadori and R. F. Frindt, *Phys. Rev.* **132**, 4893 (1970).
- ¹⁶⁴A. G. Abdullaev, I. G. Aksianov, A. I. Mamedov, and K. I. Abdullaev, *Thin Solid Films* **75**, L7 (1981).
- ¹⁶⁵L. V. Keldysh, *Pis'ma Zh. Eksp. Teor. Fiz.* **29**, 716 (1979) [*JETP Lett.* **29**, 658 (1979)].
- ¹⁶⁶C. Carlone, S. Jandle, and H. R. Shanks, *Phys. Status Solidi B* **103**, 123 (1981).
- ¹⁶⁷I. C. Irvin, R. M. Hoff, B. P. Clayman, and R. A. Bromley, *Solid State Commun.* **13**, 1537 (1973).
- ¹⁶⁸K. R. Allakhverdiev, E. Yu. Salaev, S. S. Babaev, and M. M. Tagyev, *Phys. Status Solidi B* **96**, 177 (1979).
- ¹⁶⁹R. L. Toulec, H. Piccioli, M. Mejjatti, and M. Balkanski, *Nuovo Cimento B* **38**, 159 (1977).
- ¹⁷⁰C. Herring, *J. Franklin Inst.* **2333**, 525 (1942).
- ¹⁷¹A. C. Bailey and B. Yates, *J. Appl. Phys.* **41**, 5088 (1970).
- ¹⁷²A. Bourdon, *J. Phys. (Paris) C3* **35**, 261 (1974).
- ¹⁷³J. L. Brebner, *Can. J. Phys.* **51**, 497 (1973).
- ¹⁷⁴Y. Sasaki, K. Hamaguchi, and J. Nakai, *Jpn. J. Appl. Phys.* **14**, 494 (1975).

Translated by S. Torstveit